EVALUATION OF SHIELDING EFFECTIVENESS OF A REGULARLY FILLED CONDUCTIVE COMPOSITE FOR ELECTROMAGNETIC SHIELDING

A Thesis

Submitted to the Department of Electrical and Electronic Engineering, BUET, Dhaka in partial fulfillment of the requirements for the degree

of

MASTER OF SCIENCE IN ELECTRICAL AND ELECTRONIC ENGINEERING

by

S. M. Shamim Hasan

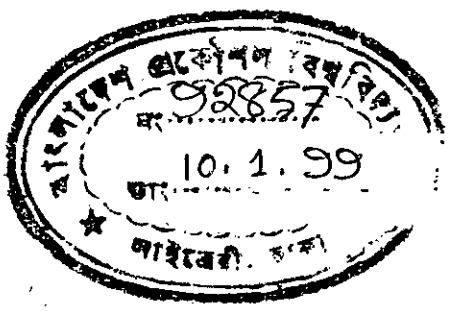

DEPARTMENT OF ELECTRICAL AND ELECTRONIC ENGINEERING

BANGLADESH UNIVERSITY OF ENGINEERING AND TECHNOLOGY

DHAKA, BANGLADESH

July, 1998

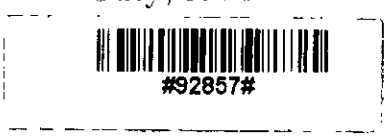

Dedicated to my parents

Mr. S. M. Abul Hossain

&

Mrs. Bil Kis Banu

CERTIFICATE

This is to certify that the work presented in this thesis was done by me under the complete supervision of **Dr. Pran Kanai Saha**, Associate Professor, Department of Electrical and Electronic Engineering, BUET, Dhaka, Bangladesh. It is also certify that this thesis work has not been submitted for the award of any degree or diploma.

Countersigned:

P.K. Saha 27/7/98
(Dr. Pran Kanai Saha)

Shamim Hasan 27/07/98
(S. M. Shamim Hasan)

The thesis titled "**EVALUATION OF SHIELDING EFFECTIVENESS OF A REGULARLY FILLED CONDUCTIVE COMPOSITE FOR ELECTROMAGNETIC SHIELDING** ", submitted by S. M. Shamim Hasan, Roll No. 930604F, Registration No. 93721, Session 1992-93-94 of M.Sc. in Engineering has been accepted as satisfactory in partial fulfillment of the requirements for the degree of

MASTER OF SCIENCE IN ELECTRICAL AND ELECTRONIC ENGINEERING

Board of Examiners

P.K.Saha 3/8/98

1. **DR. PRAN KANAI SAHA**
   Associate Professor,
   Department of Electrical & Electronic Engineering,
   BUET, Dhaka-1000.
   Chairman
   (Supervisor)

E Basher 3/8/98

2. **DR. ENAMUL BASHER**
   Professor and Head,
   Department of Electrical & Electronic Engineering,
   BUET, Dhaka-1000.
   Member
   (Ex-officio)

M. A. Matin

3. **DR. MD. ABDUL MATIN**
   Professor,
   Department of Electrical & Electronic Engineering,
   BUET, Dhaka-1000.
   Member 3.8.1998

4. **DR. MD. MORTUZA ALI**
   Assistant Professor,
   Department of Electrical & Electronic Engineering,
   BIT, Rajshahi; Rajshahi-6204.
   Member
   (External)

ACKNOWLEDGMENT

The author would like to acknowledge his sincere and profound gratitude to his advisor, Dr. Pran Kanai Saha who patiently gave many invaluable advises, continuous guidance, and constant encouragement during thesis work.

Special thanks to Prof. Dr. Md. Abdul Matin and Dr. Md. Mortuza Ali for their cooperation in many ways and for the necessary information about the research.

The author takes this opportunity to express his deepest appreciation to Dr. Enamul Basher, Professor and Head of the Department of Electrical and Electronic Engineering, BUET for providing departmental facilities. Grateful acknowledgment is also made for the research grants provided by the authority of BUET that enable the author to conduct this research.

The author would like to give thanks to Dr. Yasunory Iwanami, Associate Professor, Department of Electrical Engineering, Nagoya Institute of Technology, Japan for encouragement and sending necessary papers; to Md. Wali Ahad, Chief Engineer and to SalahUddin Ahmed, Principal Engineer, Bangladesh Atomic Energy Commission (BAEC) for their valuable suggestions and encouragement.

Special thanks is given to Dr. Madhabi Islam, Principal Scientific Officer, BAEC and to Mr. Shamsul Alam, Lecturer, Department of Mathematics, BIT, Rajshahi for their continuous supports, suggestions and encouragement.

Finally, author would like to give thanks to them who directly or indirectly helped in this research work, specially to Farhana Rahman, Engr. Kaisar Rashid Khan, Mr. Md. Jakaria Ahmed, Engr. Md. Delowar Hossain, Engr. Safat Ullah Patwari and Mr. Meraj A Mehbub-Ul-Islam.

ABSTRACT

Shielded enclosure is used with electronic equipment to fight against EMI. The level of shielding of the enclosure in preventing EMI is usually determined by the shielding effectiveness (SE) value of the material used for the enclosure.

Conductive composite plastic materials are now widely used for the shielded enclosure to reduce ingress or emission of electromagnetic interference (EMI) problem of the equipment. Two types of conductive composite are surface metallized plastic and filled composite. Filled composite is now widely used in electronic industry to combat against EMI as well as electrostatic discharge (ESD). Filled composite is a homogeneous mixture of plastic resin and conductive filler. Filler in the plastic may be arranged either in a regular form or in a random form. A regularly filled conductive composite (RFCP) is very similar to a frequency sensitive surface (FSS) which exhibits different reflection and transmission coefficient as a function of frequency.

In this research work a two dimensional periodic array of fillers (FSS) has been proposed as shielding material for making the shielded enclosure. Two types of conductive fillers (FSS elements) have been considered. The conductive fillers in the form of strip and square loop have been considered to be firmly attached to the plastic substrate. Conductive strip or square loop on a dielectric substrate constitutes an inhomogeneous medium, because electric field partly exists in the substrate and partly in the air. Thus the non-homogeneous medium has been replaced by a homogeneous medium having an effective dielectric constant. Shielding effectiveness of such type composite is mainly due to the reflection. A mathematical model has been developed to evaluate the shielding effectiveness of the strip array as well as the square loop array from the reflection coefficient. The analysis of the RFCP has been carried out by mutual impedance

method. It is observed that the frequency of the incident field, angle of incidence, RFCP (i.e. FSS) geometries, substrate material and the incident field polarization have considerable effects on the reflection coefficient of such type of RFCP. Absorption loss is available in the case of loop like filler in a plastic substrate. Absorption loss is computed from the loop resistive loss by considering the small loop approximation. Using the same type and same amount of conducting and substrate material it is found that SE value of the RFCP with square loop like filler is greater than that of the RFCP with strip like filler.

CONTENTS

	Pages
Certificate	(iii)
Board of Examiners	(iv)
Acknowledgment	(v)
Abstract	(vi)
List of Acronyms	(xii)
List of Symbols	(xiii)
List of Figures	(xv)

CHAPTER 1 GENERAL INTRODUCTION

1.1	INTRODUCTION	1
1.2	SELECTION OF ENCLOSURE MATERIAL	2
1.3	CONDUCTIVE COMPOSITE PLASTIC MATERIALS	4
	1.3.1 Surface metallized plastic	5
	1.3.2 Filled composites	6
1.4	VARIOUS TECHNIQUES FOR FSS ANALYSIS	8
1.5	AIM AND OBJECTIVES OF THE THESIS	11
1.6	ORGANIZATION OF THE THESIS	11

CHAPTER 2 THEORETICAL BACKGROUND

2.1 INTRODUCTION 12

2.2 SHIELDING EFFECTIVENESS 12

2.3 FSS AND APPLICATION 15

2.4 EFFECTIVE DIELECTRIC CONSTANT 18

2.5 SIMULATED FSS ELEMENT 20

2.6 MUTUAL IMPEDANCE METHOD 20

2.6.1 Mutual impedance 21

2.6.2 Driving point impedance 22

CHAPTER 3 MATHEMATICAL MODELING

3.1 INTRODUCTION 23

3.2 MUTUAL IMPEDANCE BETWEEN TWO DIPOLES 23

3.2.1 Self impedance 24

3.2.2 Electric field 26

3.2.3 Mutual impedance 28

3.3 MUTUAL IMPEDANCE OF THE ARRAY OF DIPOLES 30

3.4 SE OF THE ARRAY OF DIPOLES 32

3.4.1 Reflection coefficient of the array of dipoles 33

3.5 SE OF THE ARRAY OF SMALL SQUARE LOOPS 34

3.5.1 Reflection coefficient of the array of small square loops 34

3.5.1.1 Reflection coefficient of vertical array 36

3.5.1.2 Reflection coefficient of horizontal array 38

3.5.2 ABSORPTION LOSS OF THE ARRAY OF SMALL SQUARE LOOPS 39

CHAPTER 4 RESULTS AND DISCUSSIONS

4.1 INTRODUCTION 41

4.2 REFLECTION COEFFICIENT AT VARIOUS FREQUENCIES 41

4.3 EFFECT OF INCIDENCE ANGLE 42

4.4 EFFECT OF RFCP GEOMETRIES 43

4.4.1 Effect of horizontal spacing 44

4.4.2 Effect of vertical spacing 45

4.4.3 Effect of number of fillers 46

4.5 EFFECT OF DIELECTRIC SUBSTRATE 47

4.5.1 Effect of dielectric constant 47

4.5.2 Effect of substrate thickness 49

4.6 REFLECTION COEFFICIENT OF STRIP ARRAY AND SQUARE LOOP ARRAY 51

4.7 ABSORPTION LOSS OF THE SQUARE LOOP ARRAY 52

CHAPTER 5 CONCLUSION AND RECOMMENDATIONS FOR FUTURE WORK

5.1 CONCLUSION 54

5.2 RECOMMENDATIONS FOR FUTURE WORK 55

APPENDICES

Appendix A: Reflection coefficient of the array of loaded dipoles in a homogeneous dielectric medium 57

Appendix B: Angle of reflection coefficient 64

Appendix C: Relative permittivity of different dielectric materials 65

Appendix D: Relationship between the frequency at which maximum reflection is occurred and dielectric constant 66

Appendix E: Computer programs 67

REFERENCES 87

LIST OF ACRONYMS

EMC	Electromagnetic Compatibility
EMI	Electromagnetic Interference
SE	Shielding Effectiveness
FSS	Frequency Sensitive Surface
RFI	Radio Frequency Interference
FCC	Federal Communications Commission
RFCP	Regularly Filled Conductive Plastic
IL	Insertion Loss

LIST OF SYMBOLS

c	speed of light (= 3 x 10^{8} m/s)
f	frequency, Hz
β	phase constant (= $2\pi/\lambda$), rad/m
ε	permittivity, F/m
ε_r	relative permittivity, F/m
ε_{re}	effective dielectric constant , F/m
ε_0	permittivity of free space (= 8.852 x 10^{-12} F/m)
μ	permeability , H/m
μ_r	relative permeability , H/m
μ_0	permeability of free space (= 4π x 10^{-7} H/m)
λ	wave length , m
ω	angular frequency (= $2\pi f$), rad/s
ϕ	scalar potential
$\vec{A}$	vector magnetic potential
$\vec{E}$	electric field vector, V/m
ρ_l	linear charge density
u	phase velocity, m/s
SE	shielding effectiveness, dB
A	absorption loss, dB
R	reflection loss, dB

B	successive reflection loss, dB
R	Reflection coefficient, dimensionless
Z_{rk}	mutual impedance, Ω
Z_L	load impedance, Ω
Z_A	driving point impedance, Ω
ε_k	Neumann factor
l	length, m
l_e	effective length, m
ϕ_i	incidence angle, rad
σ	conductivity, mhos/m
L	loop perimeter, m
R_L	loop loss resistance, Ω
IL	insertion loss, dB
a	wire (dipole) radius, m
w	strip width, m
t	strip thickness, m
s	strip separation, m
h	substrate thickness, m
D_x	spacing between two adjacent horizontal elements, m
D_z	spacing between two adjacent vertical elements, m

LIST OF FIGURES

Pages

Fig. 1.1: FCC EMI radiation limits (Industrial and Commercial class). 2

Fig. 1.2: Levels of shielding effectiveness. 3

Fig. 1.3: Filled conductive plastic samples: (a) Regularly filled conductive composites and (b) Randomly distributed conductive fillers in plastic resin. 7

Fig. 1.4: SE expressed in the form of reflection coefficient: experimental results of the magnitude of reflection coefficient as a function of frequency of the array shown in Fig. 1.3 (a) (sample #1) and (b) (sample#2). 8

Fig. 2.1 A shield where a noise source is contained, preventing EMI with equipment outside the shield. 13

Fig. 2.2 A shield around a receptor to prevent EMI from outside world. 13

Fig. 2.3 Measuring the shielding effectiveness of a material: (a) Unloaded coupling and (b) Loaded coupling. 14

Fig. 2.4 Some typical FSS unit cell geometries: (a) Square patch, (b) Dipole, (c) Circular patch, (d) Cross dipole, (e) Square loop, (f) Circular loop, (g) Jerusalem cross and (h) Square aperture. 15

Fig. 2.5 Reflector antenna system using frequency selective screen. 16

Fig. 2.6 Spectral response of screen used in Fig.2.5. 17

Fig. 2.7 Cross sectional dimensions of coplanar strips. 18

Fig. 2.8 Field distribution for coplanar strips configuration. 19

Fig. 2.9 Replacement of an inhomogeneous dielectric with a homogeneous medium (ε_{re}). 19

Fig. 2.10 Parallel coupled antennas. 21

Fig. 2.11 Array of 2 linear $\lambda/2$ elements showing driving point. 22

Fig. 3.1 Geometry of a center fed dipole in equivalent dielectric medium (ε_{re}). 24

Fig. 3.2 Parallel coupled antennas in equivalent homogeneous dielectric medium (ε_{re}). 29

Fig. 3.3 Array of loaded dipoles in a homogeneous dielectric medium (ε_{re}) and incident EM wave with vertical polarization. 30

Fig. 3.4 Array of square loops in a homogeneous dielectric medium (ε_{re}). 35

Fig. 4.1 Reflection coefficient as a function of frequency. 42

Fig. 4.2 Reflection coefficients for various incidence angles. 43

Fig. 4.3 Reflection coefficients for different horizontal spacing. 44

Fig. 4.4 Reflection coefficients for different vertical spacing. 45

Fig. 4.5 Reflection coefficients for different number of fillers. 46

Fig. 4.6 Reflection coefficients of FSS for free standing condition and on a dielectric. 47

Fig. 4.7 Reflection coefficients for different dielectric substrate. 49

Fig. 4.8 Reflection coefficients for different substrate thickness. 50

Fig. 4.9 Reflection coefficients of strip array and square loop array. 51

Fig. 4.10 Absorption loss of the square loop array. 52

CHAPTER 1

GENERAL INTRODUCTION

- INTRODUCTION
- SELECTION OF ENCLOSURE MATERIAL
- CONDUCTIVE COMPOSITE PLASTIC MATERIALS
- VARIOUS TECHNIQUES FOR FSS ANALYSIS
- AIM AND OBJECTIVES OF THE THESIS
- ORGANIZATION OF THE THESIS

বাংলাদেশ প্রকৌশল বিশ্ববিদ্যালয়
92857
10.1.99
লাইব্রেরী, ঢাকা

1.1 INTRODUCTION

The electromagnetic environment has become polluted because of widespread proliferation of various electronic appliances and instruments in our daily life. The pollutant is the Electromagnetic Interference (EMI) both inter-device and intra-device. Electronic equipment designers and manufacturers are now very conscious to fight against EMI for complying their products with the EMC standards set by the various governmental organizations and international bodies.

The term 'shield' usually refers to a metallic enclosure that completely encloses an electronic product or a portion of that product. The propagation of electric and magnetic fields from the product to the outside and from the outside to the product can be prevented by the enclosure. Conductive composite plastic material is now being widely used for the shielded enclosure to reduce ingress or emission of electromagnetic interference (EMI) problem of the equipment [1]-[3]. Two types of conductive composite are found such as surface metallized plastic and filled composite plastic. Filled composite is now widely used in the electronic industry to combat against EMI as well as for electrostatic discharge (ESD).

The level of shielding against EMI is usually determined by the Shielding Effectiveness (SE) of the material used for the enclosure [4]. The term SE is defined as the ratio of the magnitude of the EM field that is incident on the shield to the magnitude of the EM field that is transmitted through the shield. In this work SE is evaluated for filled conductive plastic where the conductive fillers are regularly distributed in a plastic resin.

Proper selection of enclosure material is very much important for designing a shielded enclosure. Selection of the enclosure material is briefly discussed in section 1.2. Now days, conductive composites are used to cover electronic equipment to shield EMI instead of using metallic

enclosure. Conductive plastic composites and various techniques of imparting shielding capability to plastics are described in section 1.3. A comprehensive review on various techniques for analysis of FSS is given in section 1.4. Section 1.5 contains the aim and objectives of this thesis. Organization of the thesis is presented in section 1.6.

1.2 SELECTION OF ENCLOSURE MATERIAL

Various Governmental organizations and international bodies such as European Electromechanical Standardization Committee and CENELEC in Europe, Federal Communication Commissions (FCC) and the Department of Defense (DOD) in USA and the Verband Deutscher Elektrotechniker (VDE) in Germany specify the EMC requirements for various types of electronic equipment. For example, EMI radiation limits set by FCC for the industrial and commercial class of equipment is shown in Fig.1.1.

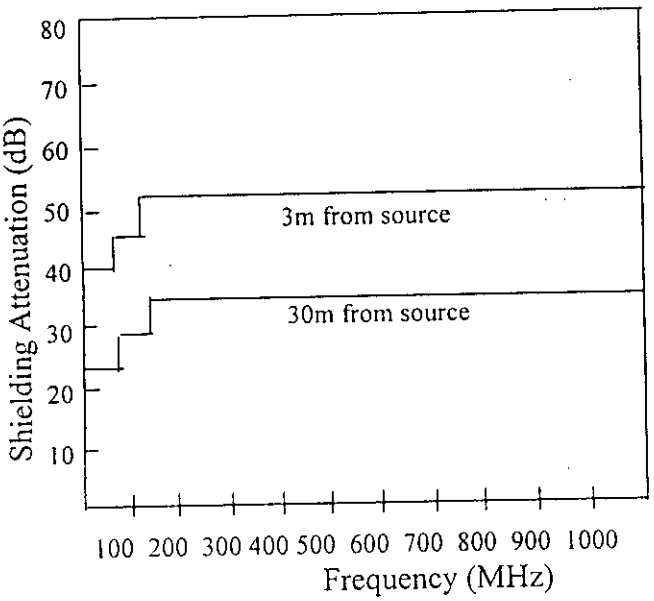

Fig 1.1 FCC EMI radiation limits (Industrial and Commercial class)[5].

The proper selection of shielding material is very important to make the enclosure for combating the electrical and electronic equipment against EMI. During designing the enclosure, aperture planning, grounding and proper joints play a vital role but it is obvious that a good quality material is a prime important factor.

Proper shielding of electronic equipment was traditionally achieved using a metallic "Faraday Cage". The designers are compelled to find out an alternative material due to high cost and heavy weight of the metal. The plastic material can be an alternative solution. But plastic does not provide any shielding capability against EMI. The technology of imparting conductivity into plastic material extends its use for EM shielding.

Conductive plastics can provide good or even excellent shielding capability. More over, these have other important features such as low cost, lightweight, easy formability and improved aesthetics. So, these have been become attractive for constructing shielded enclosure for the electronic equipment. Fig. 1.2 gives the levels of SE according to the requirement [6].

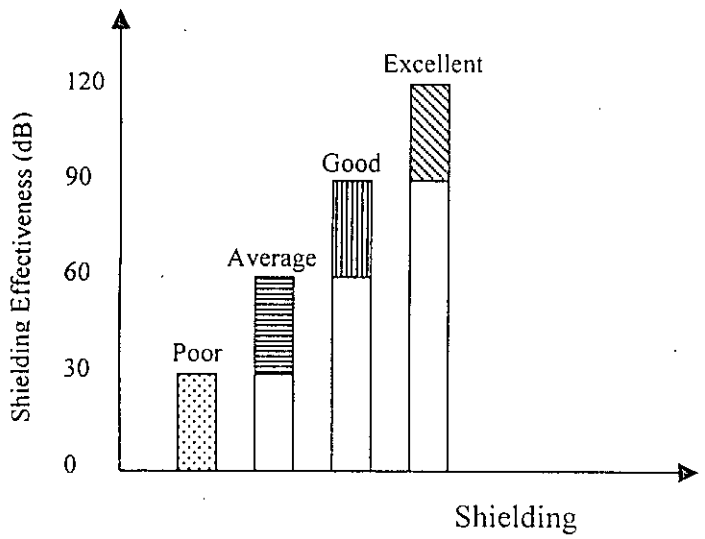

Fig.1.2 Levels of shielding effectiveness.

Various techniques of imparting conductivity to plastic materials are discussed in the next section.

1.3 CONDUCTIVE COMPOSITE PLASTIC MATERIALS

Plastic materials, which are commonly used as the polymeric resin (dielectric substrate), are: polycarbonate, ABS (Acrylonitrile Butadiene Styrene), polystyrene, nylon, polyethylene, polypropylene and maleated polystyrene (SMA) co-polymer. A number of techniques are available to impart conductivity in plastics. According to the method of imparting conductivity into plastic, these can be classified as: (i) Surface Metallized Plastic and (ii) Filled Composite. These two types of composite plastic are described in the following subsections. A comparative study of different metallization techniques for plastics is given in Table I.

Table I: A comparative study of different metallization techniques for plastics [7].

Techniques	Shielding effectiveness (dB)	Uses
Electroless plating	70-120	For military purpose or for sophisticated shielding.
Arc spraying	60-90	Use has been limited now a day.
Vacuum metallization	40-70	For low frequency shielding.
Conductive paints	30-70	For data processing equipment, computer etc.
Conductive composite	30-60	For computational equipment and information related apparatus etc.
Conductive fabrics	40-100	For bonding straps, cable shielding etc.
Flexible laminates	60-100	For keyboard, printers etc.

1.3.1 Surface metallized plastic

In the case of **Surface metallized plastic,** the plastic surface (usually the inner surface, when it is used for enclosure) is coated by using metal (such as copper, nickel, aluminium etc.). Various techniques for surface metallization of plastic materials include: (i) conductive painting, (ii) arc spraying, (iii) electroless plating and (iv) vacuum metallization. Flexible laminates and conductive fabrics can also be used for making the shielded enclosure. The metallization techniques are briefly discussed below.

Conductive Paint has solids' content, which is composed of binders (e.g. acrylic, urethane) and electroconductive fillers (e.g. copper, silver, graphite, nickel) in the form of powder. In this technique conventional paint spraying equipment can be used for painting a plastic substrate. The value of SE depends on the paint thickness and the type of conductive material.

In **Electroless Plating** method, a film of pure homogeneous metal whose thickness can be varied from 0.25 micron to 1.0 micron is deposited on a plastic substrate. It depends on the immersion of the substrate in a series of chemical solutions to produce metal plating by autocatalytic means instead of dc current [8]. Copper and nickel are generally used as a metal for plating and excellent SE values could be achieved. SE value depends on the metal used and the thickness of the plating.

Vacuum Metallization involves deposition of an extremely thin metallic film (generally aluminium) on a plastic substrate by evaporation method in a high vacuum chamber. The vaporization is achieved by energizing tungsten filaments with high current, where, excessive heat is generated and pellets of metals (usually aluminium) are converted into gaseous form. The aluminium gas particles have sufficient kinetic energy to generate high velocities, which when

applied to the plastic substrate produce both a chemical and a mechanical bond. Aluminium layer thickness range from 0.5-25 μ m.

In **Arc Spraying**, the pure metal (generally zinc) is melted by electric arc and is propelled by compressed air for spraying droplets of molten metal onto the part to be coated [9], [10]. Coating thickness varies from 0.05 mm to 0.075 mm.

Laminates of metal foil (usually aluminium and copper) bonded to a reinforcing substrate (e.g. polyester, PVC, polyamide etc.) are now being used as an integral part of the EMC of a unit or a building [11] which are termed as **Flexible Laminates**. The SE of such materials essentially depends on the thickness and conductivity of the metal foil used.

Conductive fabrics are fine wires of solid metals (e.g. nickel, copper, silver and gold) woven, knitted or formed into sheets to be glued with fabrics (e.g. polyester. Polyamide, rayon). Conductive fabrics can be used for imparting shielding capability to plastics in lieu of conductive paints or other metallic coating [7].

1.3.2 Filled composites

Filled Composite Plastic is a homogeneous mixture of plastic resin and conductive filler, usually metal or carbon. The most widely used conductive fillers in the form of flake or fibre are graphite, copper, aluminium, stainless steel, nickel and nickel coated carbon. SE depends on the type and amount of conductive filler added to the plastic. Filler in the plastic may be arranged either in the regular form or in random form as shown in Fig.1.3. A regular array of conductive flakes in a plastic resin is very similar to a frequency sensitive surface (FSS).

Filled composites are widely used in the electronic industry for electrostatic discharge (ESD) protection in silicon chip storage bins, anti static floor mats, handling gloves and wrist straps which ground any build up of static electricity. They are also used for shielding of computational equipment and information related apparatus.

Regularly Filled Conductive Composites (RFCP) is a two dimensional regular array of conductive flakes in the plastic resin. This can be termed as Frequency Sensitive Surface (FSS). A FSS is a surface, which exhibits different reflection or transmission coefficients as a function of frequency. Usually a FSS consists of identical antenna elements such as dipoles. When the elements resonate and the resistive part of the load connected to each of the array elements is zero then the array can provide complete reflection.

Although RFCP acts as FSS (i.e. this type of material is frequency sensitive), its bandwidth of high reflectivity to EM waves can be widened by manipulating the dipole size and separation. This design flexibility would be an added advantage of these composites.

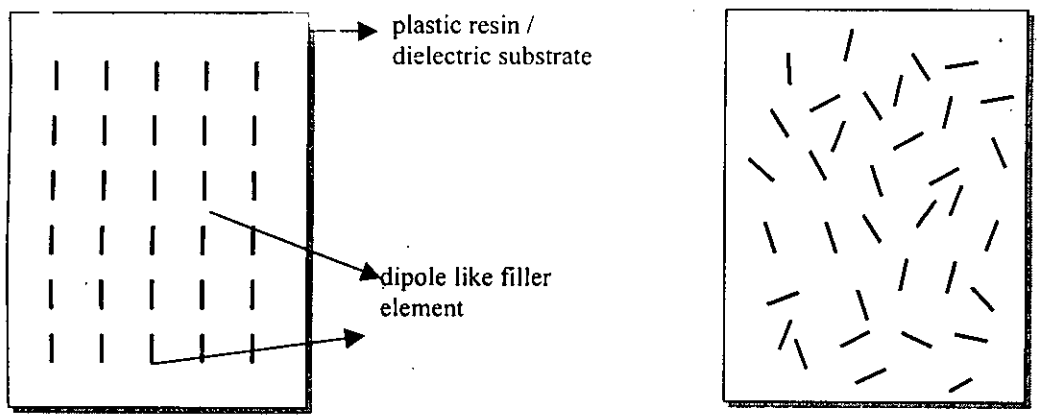

Fig.1.3 Filled conductive plastic samples: (a) Regularly filled conductive composites, (b) Randomly distributed conductive fillers in plastic resin.

Experimental results showed that the SE of RFCP is better than that of randomly distributed conductive fillers in plastic resin [12]. This is shown in Fig. 1.4.

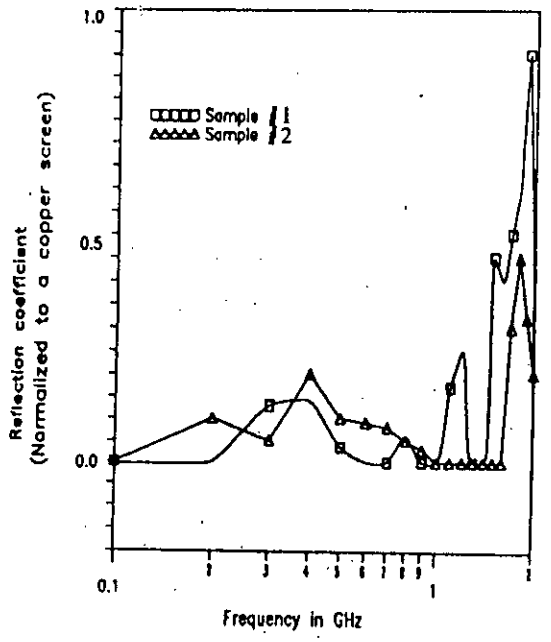

Fig.1.4 SE expressed in the form of reflection coefficient: experimental results of the magnitude of reflection coefficient as a function of frequency of the arrays shown in Fig.1.3 (a) (sample # 1) and (b) (sample # 2)[12].

1.4 VARIOUS TECHNIQUES FOR FSS ANALYSIS

Five different techniques that can be employed to analyze periodic scattering arrays or FSSs. These are as follows: (i) variational method (ii) point matching method (iii) mutual impedance method (iv) modal matching method and (v) spectral domain analysis method.

R.B. Keiburtz [13] proposed **variational method** to analyze an FSS of conducting thin screen perforated with square holes. The transmission coefficient for normal incidence of plane wave on FSS was evaluated in this technique. Accuracy of this method is poor and that depends on the ability to choose an approximate trial function. Method of calculation in this technique is complicated and analysis can be done only for normal incidence for periodic array of aperture in a conducting screen.

Ott et al.[14] applied a **point matching technique** to derive the reflection and transmission coefficient of a periodic planar array of dipoles for normal incidence. This method is also complicated and the accuracy is not satisfactory. Though this method can be employed for calculating the reflection and transmission coefficient of a periodic array of dipoles, this can be used to analyze the problem only for normal incidence.

Later this analysis was simplified by Munk et al. [15] by assuming the elements of the array as antennas. The reflection coefficient was determined in terms of the driving point impedance of individual elements. As in this method, mutual effect of all the elements of the array are considered in calculating the driving point impedance, it is known as **mutual impedance method.** Normal incidence as well as non-normal incidence were covered in this analysis.

The **modal matching technique** has been discussed in detail by a number of authors [16], [17]. In this technique starting from the Floquet mode vector for TE and TM modes, the mode vectors are computed for E- and H-fields, from which then the modal impedance is computed. The incident and specularly reflected waves are then expressed in terms of unknown modal coefficients; applying the boundary condition of zero tangential E-field in the conducting portion of FSS, these coefficients can then be evaluated. Assumption of symmetric and anti symmetric excitation would make the analysis simpler and free space reflection coefficient can be expressed

in terms of symmetric and antisymmetric reflection coefficients. This modal matching technique can be carried out for the analysis of a FSS of thick slot or the complementary problem of thick conducting strips embedded in dielectric. The accuracy of the solution depends upon the number of modes used to approximate the aperture or strip field distribution. This technique is more complicated than the mutual impedance method.

The **spectral domain analysis** is more involved since it deals with the fields scattered from the FSS in terms of the unknown induced current on the conducting part of it. The periodicity of the geometry of FSS is exploited by writing the scattered field equations in the Fourier integral form. These integral equations are then solved for the unknown induced current by using the method of moments. Hence, the above mentioned coefficients can be easily determined through a set of simple algebraic relations from the knowledge of the scattered field. A detailed analysis can be found in [18]-[20]. The accuracy of spectral domain analysis is very high but it largely depends upon the proper choice of basis and testing functions which is very difficult to choose for a particular problem. The computation by using this technique is time consuming.

In the present research work, mutual impedance method is used for finding the shielding effectiveness of FSS of dipole like fillers and small square loop like fillers as it possesses some advantages over other methods. This technique is very simple and amenable. This technique requires less computational time and can be readily extended to more general array configurations. The analysis can be done for different incidence angle of the EM wave.

1.5 AIM AND OBJECTIVES OF THE THESIS

This research work is aimed at developing a mathematical model to evaluate the shielding effectiveness of FSS like conductive composite plastic material. To achieve this aim the following objectives were envisaged.

- Development of a mathematical model for determining the mutual impedance of the array of loaded dipole like fillers on a dielectric substrate using induced emf method.
- Evaluation of shielding effectiveness in the form of reflection coefficient of the array of loaded dipole like fillers on a dielectric substrate using mutual impedance method.
- Development of a mathematical model for determining the reflection coefficient and absorption loss of the array of small square loop like fillers on a dielectric substrate.
- Evaluation of reflection coefficient and absorption loss of the array of small square loop like fillers on a dielectric substrate.
- Comparison of the shielding effectiveness of the dipole like filler array on a dielectric substrate with that of the small square loop like filler array.

1.6 ORGANIZATION OF THE THESIS

The thesis is organized as follow.

Theoretical background of the thesis is given in chapter 2. Frequency selective surface and it's application, shielding effectiveness and effective dielectric constant of the medium surrounding conductive fillers are described in this chapter. Chapter 3 contains the mathematical model to evaluate the shielding effectiveness of FSSs both for dipole like fillers and small square loop like fillers on a dielectric substrate. Results and discussion are given in chapter 4. Chapter 5 contains the conclusion and recommendations for further research.

CHAPTER 2

THEORETICAL BACKGROUND

- INTRODUCTION
- SHIELDING EFFECTIVENESS
- FSS AND APPLICATION
- EFFECTIVE DIELECTRIC CONSTANT
- SIMULATED FSS ELEMENT
- MUTUAL IMPEDANCE METHOD

2.1 INTRODUCTION

Enclosing the electronic equipment can prevent unwanted emissions from the equipment itself as well as can protect the equipment from any other EM interference from its neighbours. The level of shielding of the enclosure is generally determined by shielding effectiveness (SE) of the material used for the enclosure. The determination of SE of any material is given in section 2.2. In this work, regularly filled composite material, which is similar to FSS is proposed for EM shielding in the microwave range of frequency. A general discussion on FSS and its application are given in section 2.3.

The FSS is considered to be placing identical elements such as dipole like filler and square loop like filler on a plastic substrate. The medium surrounding the FSS elements is inhomogeneous (air and plastic substrate). This inhomogeneous medium can be replaced by an equivalent homogeneous medium having an effective dielectric constant. The effective dielectric constant is given in section 2.4. The FSS elements on the dielectric substrate are of rectangular cross section. These elements can be replaced by equivalent wire of circular cross section. The simulated FSS element is given in section 2.5. The SE of FSS like material is computed by mutual impedance method. Method of computation of mutual impedance is described in section 2.6.

2.2 SHIELDING EFFECTIVENESS

A shield is a metallic partition placed between two regions of space as shown in Fig. 2.1 and Fig.2.2. It is used to control the propagation of electric and magnetic fields from one region to the other.

Fig.2.1 A shield where a noise source is contained, preventing EMI with equipment outside the shield.

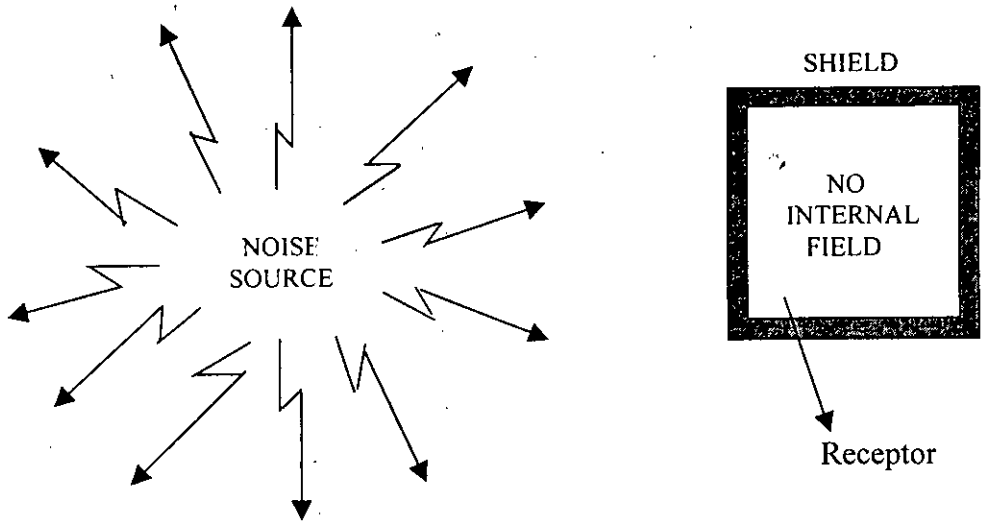

Fig.2.2 A Shield around a receptor to prevent EMI from outside world.

The term " Shielding Effectiveness (or insertion loss) " refers to the ability of a material to guard against EMI, both against emission and susceptibility. SE also relates to the ability of a material to reduce the transmission of propagating fields in order to electromagnetically isolate one region from another.

SE or insertion loss (IL) is the ratio of the signal received (from a transmitter) without the shield and to the signal received with the shield. The SE or insertion loss can be expressed as follow [21].

$$SE = IL = 10\log_{10}\frac{P_r}{P_r'} \quad dB \tag{2.1}$$

Where, P_r is the received signal strength without the shield and P_r' is the received signal strength with the shield.

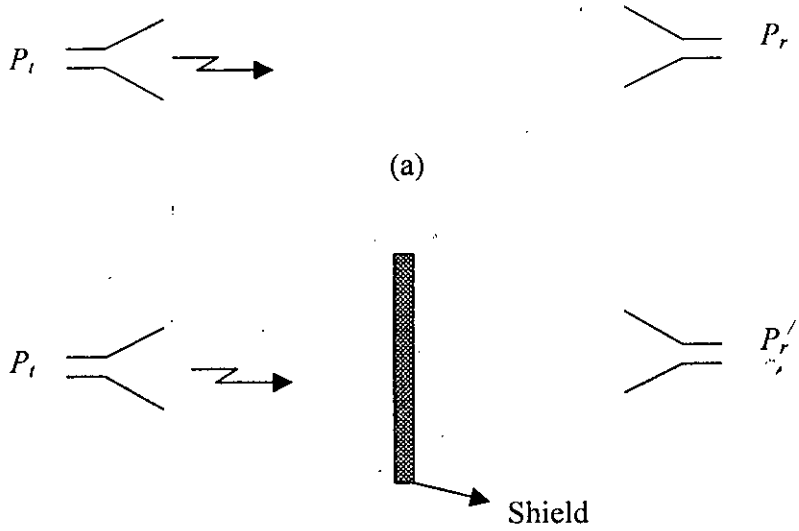

Fig.2.3 Measuring the shielding effectiveness of a material: (a) Unloaded coupling, (b) Loaded coupling [21].

Shielding effectiveness of a material can also be expressed as follow [12].

$$SE = A + R + B \quad dB \tag{2.2}$$

Where, A is the absorption loss (dB) of the material, R is the reflection loss (dB) and B is the successive reflection loss (dB) inside the material, which is negligible in most cases for electrically thin materials.

In the present case, regularly filled conductive composite (RFCP) with strip like filler (i.e. an array of strips on plastic substrate), SE is only due to the reflection loss(R), whereas the SE value of RFCP with square loop like filler will be due to the reflection and absorption losses.

Shielding effectiveness varies with frequency, geometry of the shield, position within the shield where the field is measured, type of the field being attenuated, direction of incidence and polarisation.

2.3 FSS AND APPLICATION

A FSS (Frequency Sensitive Surface) is a surface, which exhibits different reflection or transmission coefficients as a function of frequency. FSS consists of identical antenna elements such as thin dipole, rectangular patch (various aspect ratio), crossed dipole, Jerusalem cross, circular patch, triangular patch, circular loop, triangular loop and rectangular loop. These elements are shown in Fig.2.4.

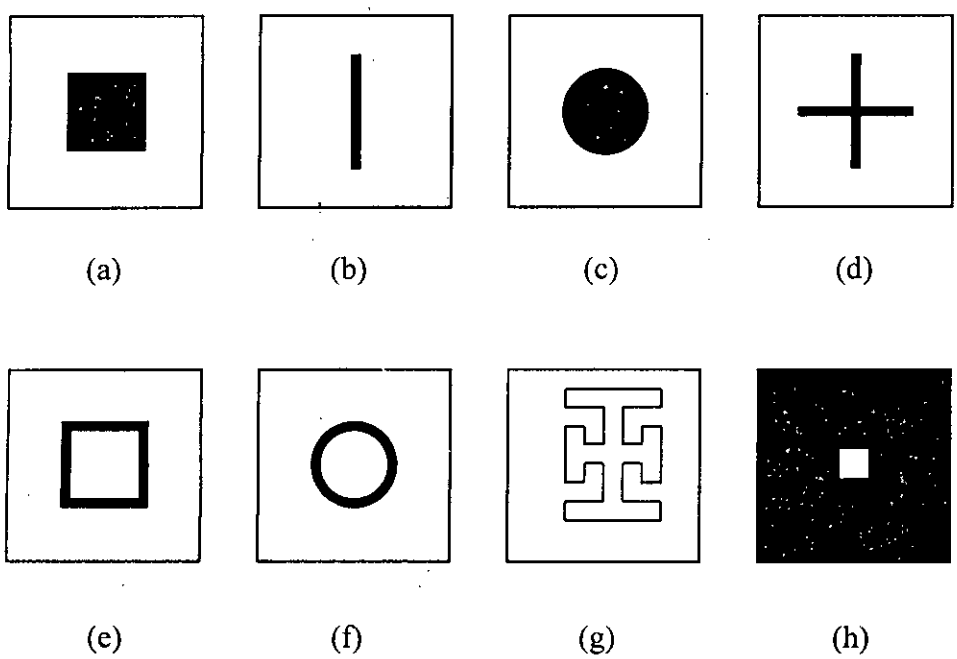

Fig.2.4 Some typical FSS unit cell geometries: (a) Square patch, (b) Dipole, (c) Circular patch, (d) Cross dipole, (e) Square loop, (f) Circular loop, (g) Jerusalem cross and (h) Square aperture [19].

In the present analysis two types of antenna elements are considered for RFSP (i.e. FSS) such as: (i) dipole like strip and (ii) small square loop. These elements are considered to avoid complexity in the analysis. Less material requirement and easy formability are also the additional advantages to consider these elements.

Frequency selective surfaces have many applications and cover most of the electromagnetic spectrum. For example, in microwave region, the frequency selective properties of periodic screen are exploited to make a more efficient use of reflector antennas [22]. As shown in Fig.2.5, a frequency selective surface is placed between two feeds, radiating at different frequencies, and the main reflector.

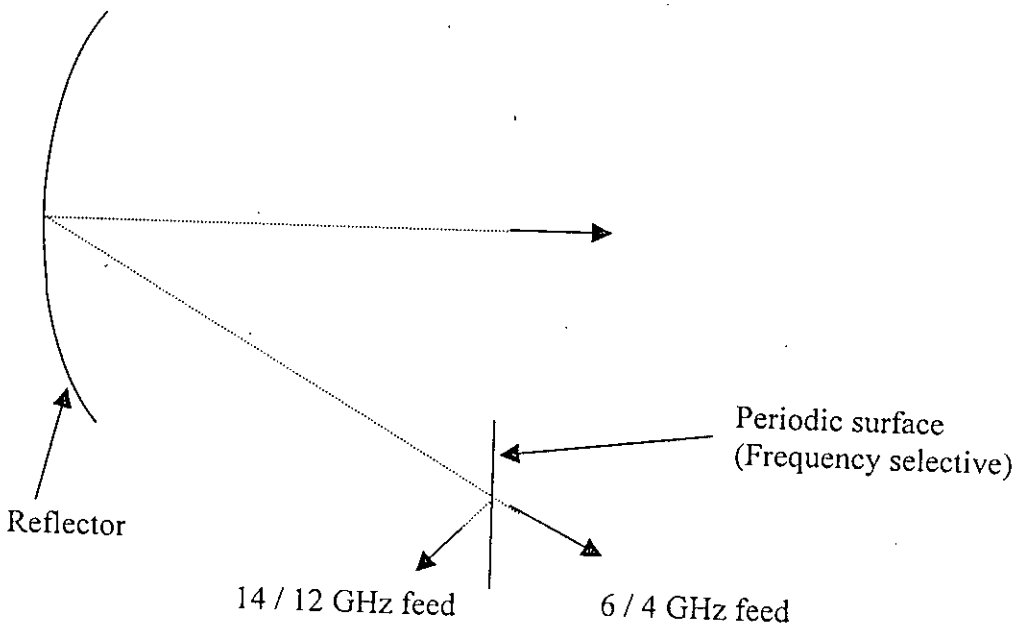

Fig.2.5 Reflector antenna system using frequency selective screen [19].

The screen is totally reflecting (or near so) over the operating band of feed one, and conversely, it is nearly totally transparent over the band of feed two. Hence, in this configuration , two independent feeds may share the same reflector antenna simultaneously, in a frequency reuse

mode. The desired spectral response of the screen is shown in Fig.2.6 for a specific incidence angle and incident field polarisation.

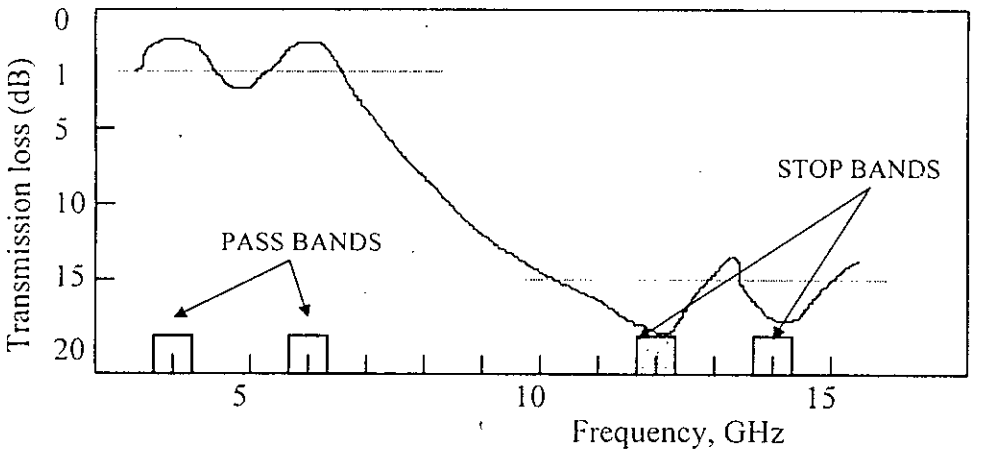

Fig.2.6 Spectral response of screen used in Fig.2.5 [19].

In the far-infrared region, periodic screens (i.e. FSSs) are used as polarizers, beam splitters, as well as mirrors for improving the pumping efficiency in molecular lasers. Another application of the FSS in this wavelength range is in infrared sensors.

In the near-infrared and visible portions of the spectrum, periodic screens can be used as solar selective surfaces to aid in the collection of solar energy.

By exploiting the benefits of FSS (such as reflection), electronic equipment can be protected from external electromagnetic disturbances as well as can also be prevented from radiating of any electromagnetic field to the EM environment.

2.4 EFFECTIVE DIELECTRIC CONSTANT

In the present case, the FSS is made by etching strips or square loops on the dielectric substrate or by embedding strips or loops between two dielectric substrates. This is very similar to the coplanar strips configuration as shown in Fig. 2.7.

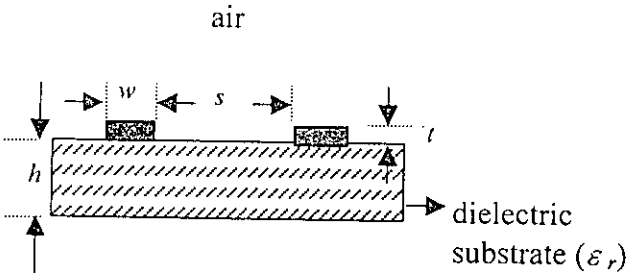

Fig.2.7 Cross sectional dimensions of coplanar strips [2].

The medium surrounding the conductive filler (strip) is referred to as an inhomogeneous medium since the electric field exists partly in the board substrate and partly in the air surrounding the board as illustrated in Fig.2.8. The effective dielectric constant (ε_{re}) is that of a fictitious dielectric material such that if the original strips are immersed in a homogeneous material having this dielectric constant as shown in Fig.2.9, the corresponding field lines in Fig.2.8 and Fig.2.9 will have the same characteristic impedance and the same velocity of propagation. This effective dielectric constant depends on the dielectric constant of the substrate (ε_r), substrate thickness (h), strip width (w), strip separation (s) and strip thickness (t).

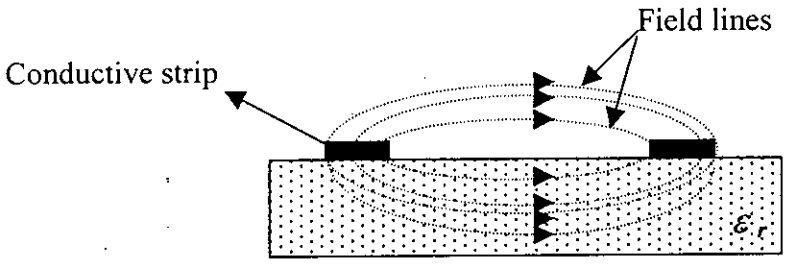

Fig.2.8 Field distribution for coplanar strips configuration[2].

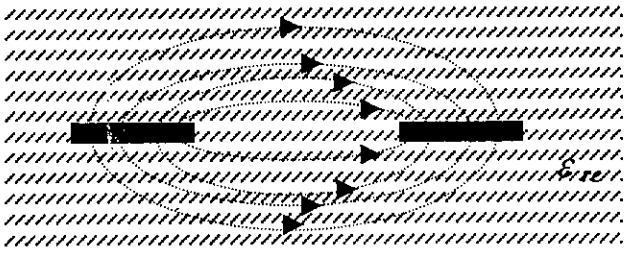

Fig.2.9 Replacement of an inhomogeneous dielectric with a homogeneous medium (ε_{re}) [2].

The dielectric substrate does not affect magnetic field because the permeability of the dielectric substrate is same as that of the air, μ_0. The effective dielectric constant (ε_{re}) for coplanar strips configuration is given as [2].

$$\varepsilon_{re} = \frac{\varepsilon_r + 1}{2}\left\{ \tan h\left[0.775 \ln\left(\frac{h}{w}\right) + 1.75\right] + \frac{kw}{h}\left[0.04 - 0.7k + 0.01(1.0 - 0.1\varepsilon_r)(0.25 + k)\right]\right\} \quad (2.3)$$

where $k = \frac{s}{s + 2w}$

2.5 SIMULATED FSS ELEMENT

In this work two types of elements (dipole like strip and small square loop like filler) are considered as FSS elements as mentioned in section 2.3. The strip attached to the dielectric substrate is of rectangular cross section. This rectangular cross section strip can be replaced by equivalent wire of circular cross section. The equivalent wire radius can be found as follow [23].

$$a = 0.335\, w\left(0.8 + \frac{t}{w}\right) \tag{2.4}$$

where a is the wire radius, w is the strip width and t is the strip thickness.

Eqn. (2.4) is valid for $0.1 < t/w < 0.8$. For a very thin rectangular strip (i.e. $0 \le t/w \le 0.1$) the equivalent wire radius can be determined from the following expression [23].

$$\mathrm{a} \approx 0.25\ \mathrm{w}\left[1 + \frac{t}{\pi w}\left(1 + \log_e\left(4\pi \frac{w}{t}\right)\right)\right] \tag{2.5}$$

2.6 MUTUAL IMPEDANCE METHOD

The present analysis for the FSS of a two dimensional regular array of conductive fillers (in the form of strips as well as small square loop) is done by mutual impedance method.

In determining the shielding effectiveness (SE) of such a FSS, the array elements are considered to be as antennas. The mutual impedance for each element of the array is computed by using induced emf method. The driving point impedance is computed from individual impedance. The reflection coefficient is then determined from driving point impedance and mutual impedance.

The same analysis is extended to find the reflection coefficient of FSS with small square loops, which are considered to be as an array of infinitesimal dipoles (i.e. strips). In the square loop like filler in plastic resin absorption loss is available. The SE of such type of conductive plastic composite is due to the reflection loss and absorption loss.

2.6.1 Mutual impedance

The mutual impedance can be defined as the impedance between any two terminal pairs in a multi element array antenna is equal to the open-circuit voltage produced at the first terminal pair divided by the current supplied to the second when all other terminal pairs are open-circuited [24].

From the circuit theory point of view, the mutual impedance of two coupled circuit is defined as the negative ratio of emf V_{21} induced in circuit-2 to the current I_1 flowing in circuit-1 with circuit-2 open. Instead of two coupled circuits, two coupled antennas, antenna 1 and 2 as shown in Fig.2.10, are considered to find the mutual impedance.

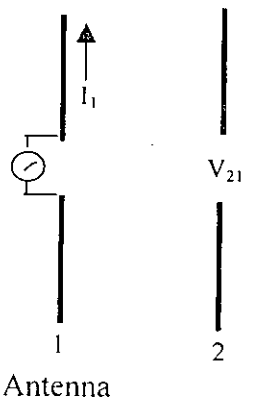

Fig.2.10 Parallel coupled antennas.

The mutual impedance Z_{21} is then,

$$Z_{21} = -\frac{V_{21}}{I_1} \tag{2.6}$$

where V_{21} is the emf induced across the terminals of the open-circuited antenna 2 by the current I_1 in the antenna 1.

2.6.2 Driving point impedance

Driving point impedance at any pair of terminals can be defined as the ratio of an applied potential difference to the resultant current at these terminals with all terminals are terminated in any specified manner [24].

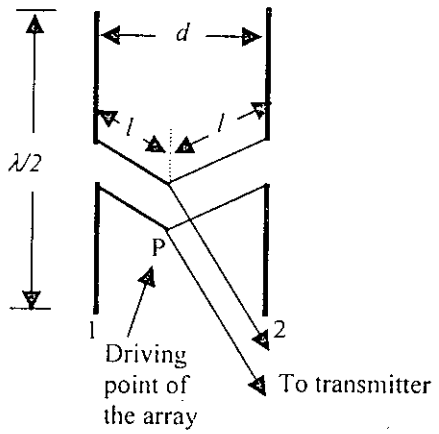

Fig.2.11 Array of 2 linear $\lambda/2$ elements showing driving point [3].

Two transmission lines of equal length l is connected at point P and then is extended to a third line extending to a transmitter is shown in Fig. 2.11 above to explain the driving point impedance. Point P is called driving point and the impedance at this point is called driving point impedance.

CHAPTER 3

MATHEMATICAL MODELING

- INTRODUCTION
- MUTUAL IMPEDANCE BETWEEN TWO DIPOLES
- MUTUAL IMPEDANCE OF THE ARRAY OF DIPOLES
- SE OF THE ARRAY OF DIPOLES
- SE OF THE ARRAY OF SQUARE LOOPS

3.1 INTRODUCTION

A regular array of conductive strips in a plastic resin, which is very similar to a FSS, has been proposed as a shielding material for the equipment enclosure. The SE value of such type of material (FSS) is evaluated by mutual impedance method.

The dipole like strip on the dielectric substrate constitutes a non-homogeneous medium. This non-homogeneous medium can be replaced by an equivalent homogeneous medium having an effective dielectric constant (ε_{re}) as described in section 2.4. Mathematical model of mutual impedance between two dipoles on a dielectric substrate has been derived in section 3.2. The model is then extended for finding the mutual impedance of a two-dimensional periodic array of dipoles (strips) on the substrate. This has been described in section 3.3. Reflection coefficient of RFCP (FSS) has been derived from mutual impedance and driving point impedance which has been given in section 3.4.

Square loop like filler is also to be considered in a plastic resin for developing the RFCP. The same process is extended for finding the reflection coefficient for such RFCP and is given in section 3.5. Absorption loss of such type of RFCP is also derived in section 3.5. The SE of RFCP with loop like filler is due to the reflection loss and the absorption loss.

3.2 MUTUAL IMPEDANCE BETWEEN TWO DIPOLES

Induced emf method [25] can be used to find the mutual impedance of a doubly periodic array of dipoles on a dielectric substrate. This method is also employed to evaluate the self-impedance of a thin linear antenna of radius 'a' on a dielectric substrate.

3.2.1 Self impedance

The geometry of a center-fed dipole in an equivalent homogeneous medium having an effective dielectric constant (ε_{re}, refers to eqn. 2.3) is shown in Fig.3.1. The dipole shown in Fig.3.1 is assumed to be the z directed dipole in the rectangular coordinate system and P (ρ, φ, z) is the observation point in the cylindrical coordinate system.

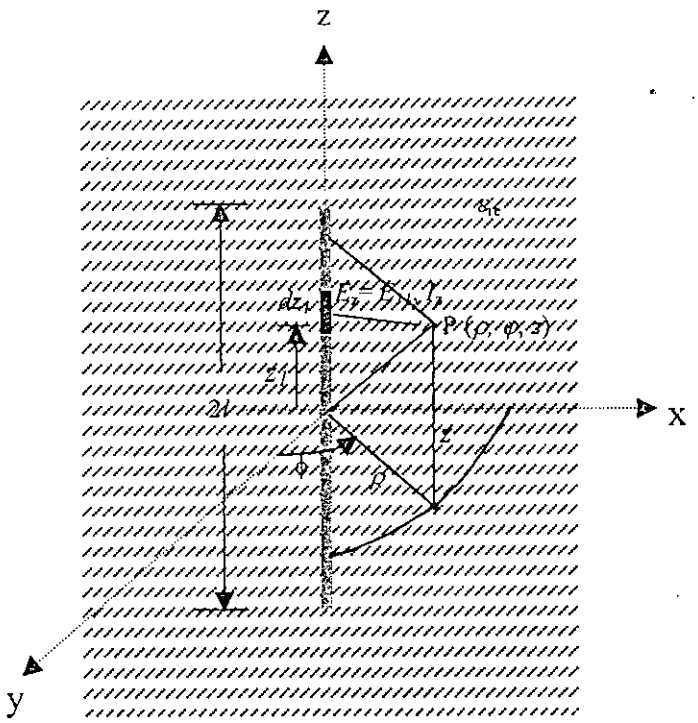

Fig.3.1 Geometry of center fed dipole in equivalent dielectric medium (ε_{re}).

Dipole length ($2l$) is considered as $m\lambda/2$ for symmetrical current distribution along the dipole, where m is an odd integer (i.e. m = 1, 3, 5 .....). A sinusoidal current distribution is assumed along the dipole. The current (I_z) at a distance z from the origin is given as.

$$I_z = I_1 \sin\beta z \tag{3.1}$$

A differential length dz_1 of the dipole at a distance z_1 from the origin along the z-axis is taken to find the self-impedance of the dipole. The self-impedance can be written as

$$Z_{11} = \frac{V_{11}}{I_1} \tag{3.2}$$

where V_{11} is the applied voltage to the antenna and I_1 is the total antenna current.

The impedance Z_{11} is constant and is independent of the current amplitude [3]. This is due to the fact that the system is linear. Thus Z_{11} can also be expressed as

$$Z_{11} = \frac{V_{11}}{I_1} = \frac{dV_{11}}{dI_1} \tag{3.3}$$

where dV_{11} is the voltage across infinitesimal element dz_1 and $dI_1$is the current flowing through the infinitesimal element of the dipole.

In this work the dipole acts as a receiving antenna and it is assumed that the reciprocity theorem holds for the present case. The eqn. 3.3 can be written as [3].

$$Z_{11} = -\frac{1}{I_1}\int_{-l}^{+l} E_{11} \sin\beta z \, dz \tag{3.4}$$

where E_{tl} is the incident electric field on the dipole at point z_l along the z-axis. The incident field is evaluated from the vector and scalar potential.

3.2.2 Electric field

The electric field is derived from the vector and scalar potential by using the following equation [27].

$$\vec{E} = -\Delta\phi - j\omega\vec{A} \tag{3.5}$$

where ϕ is the retarded scalar potential due to the charges on the antenna and $\vec{A}$ is the retarded vector potential due to the currents on the antenna.

Since the dipole is z directed in the rectangular coordinate system as shown in Fig. 3.1, only z component of the vector potential (A_z) is available. For the case of a thin dipole (wire) of length $2l$, this vector potential can be written as follows.

$$A_z = \frac{\mu}{4\pi}\int_{-l}^{+l}\frac{[I_{zl}]}{r}dz_l \tag{3.6}$$

Where, $[I_{zl}]$ is the retarded current along the dipole (wire) which can be expressed as follow [3].

$$[I_{zl}] = I_1 \sin\beta z\, e^{j\omega[t-(r/u)]} \tag{3.7}$$

where u is the phase velocity of the electromagnetic wave in the equivalent homogeneous medium and it is $\frac{1}{\sqrt{\varepsilon_{r_e}}}$ times of the velocity of the wave in free space (c), r is the distance between the source point and the observation point. The distance (r) is found to be as

$$r = \sqrt{\rho^2 + (z - z_1)^2}$$

Substituting eqn. 3.7 into eqn. 3.6, the z component of the retarded vector potential yields as,

$$A_z = \frac{\mu I_1 e^{j\omega t}}{4\pi} \int_{-l}^{+l} \frac{\sin \beta z_1 \, e^{-j\beta r}}{r} dz_1 \tag{3.8}$$

For the case of a z directed thin dipole (wire) of length *2l*, scalar magnetic potential (ϕ) can be written as follow.

$$\phi = \frac{1}{4\pi\varepsilon} \int_{-l}^{+l} \frac{[\rho_l]}{r} dz_1 \tag{3.9}$$

Where $[\rho_l]$ is the retarded linear charge density on the dipole (wire) and it can be expressed as follows [3].

$$[\rho_l] = \frac{j\beta I_1}{\omega} \cos \beta z_1 \, e^{j\omega[t-(r/u)]} \tag{3.10}$$

Substituting eqn. 3.10 into eqn. 3.9, the retarded scalar potential becomes as

$$\phi = \frac{j\beta I_1 e^{j\omega t}}{4\pi\varepsilon\omega} \int_{-l}^{+l} \frac{\cos \beta z_1 \, e^{-j\beta r}}{r} dz_1 \tag{3.11}$$

Applying De Moivre's theorem to eqn. 3.8 and eqn. 3.11, the scalar potential (ϕ) and vector potential (A_z) become as follow.

$$\phi = \frac{j\beta I_1 e^{j\omega t}}{8\pi\varepsilon\omega} \int_{-l}^{+l} \frac{e^{-j\beta(z_1+r)} + e^{j\beta(z_1-r)}}{r} dz_1 \tag{3.12}$$

$$A_z = \frac{j\mu I_1 e^{j\omega t}}{8\pi} \int_{-l}^{+l} \frac{e^{-j\beta(z_1+r)} - e^{j\beta(z_1-r)}}{r} dz_1 \tag{3.13}$$

For the z directed dipole in the rectangular coordinate system only z component of electric field ($\vec{E}$) exists and this can be written as

$$E_z = -\frac{\partial \phi}{\partial z} - j\omega A_z \tag{3.14}$$

Substituting eqns. 3.12 and eqn. 3.13 into eqn. 3.14 and considering the time factor equals to its absolute value $e^{j\omega t} = 1$, the z component of the electric field can be expressed as

$$E_z = \frac{-j\beta I_1}{8\pi\varepsilon\omega} \int_{-l}^{+l} \frac{\partial}{\partial z}\left(\frac{e^{-j\beta(z_1+r)} + e^{j\beta(z_1-r)}}{r} \right) dz_1$$

$$+ \frac{\omega\mu I_1}{8\pi} \int_{-l}^{+l} \left(\frac{e^{-j\beta(z_1+r)} - e^{j\beta(z_1-r)}}{r} \right) dz_1 \tag{3.15}$$

By equating $E_z = E_{11}$ and substituting eqn. 3.15 into eqn. 3.4, the self-impedance of the dipole (wire) in the equivalent homogeneous medium (ε_{re}) can be evaluated.

3.2.3 Mutual impedance

The mutual impedance between two-coupled dipole antennas (antenna # 1 and antenna # 2) as shown in Fig.3.2 in the equivalent homogeneous medium (ε_{re}) can be expressed as follow [3].

$$Z_{21} = -\frac{V_{21}}{I_1} = -\frac{1}{I_1}\int_{-l}^{+l} E_{21} \sin\beta z \, dz \qquad (3.16)$$

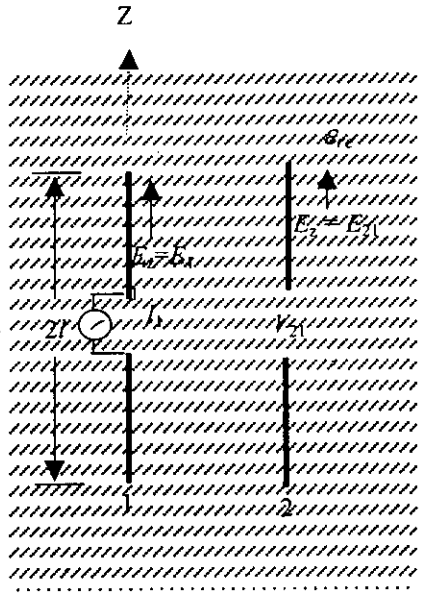

Fig.3.2 Parallel coupled antennas in equivalent homogeneous dielectric medium (ε_{re}).

where V_{21} is the induced emf in antenna # 2 due to the current I_1 in the antenna # 1.

By equating $E_{21} = E_z$ and by substituting eqn. 3.15 into eqn. 3.16, the mutual impedance between two dipole antennas (strips) in a homogeneous medium having an effective dielectric constant (ε_{re}) becomes as follow.

$$Z_{21} = \frac{j\beta}{8\pi\varepsilon\omega}\int_{-l}^{+l}\Big[\sin\beta z \int_{-l}^{+l}\frac{\partial}{\partial z}\Big(\frac{e^{-j\beta(z_1+r)} + e^{j\beta(z_1-r)}}{r}\Big)dz_1\Big]dz$$

$$-\frac{\omega\mu}{8\pi}\int_{-l}^{+l}\Big[\sin\beta z \int_{-l}^{+l}\Big(\frac{e^{-j\beta(z_1+r)} - e^{j\beta(z_1-r)}}{r}\Big)dz_1\Big]dz \qquad (3.17)$$

3.3 MUTUAL IMPEDANCE OF THE ARRAY OF DIPOLES

A doubly periodic array of thin dipoles in an equivalent homogeneous medium having an effective dielectric constant (ε_{re}) is shown in Fig.3.3. The array is placed in the x-z plane of the rectangular coordinate system. The array consists of $2R''+1$ number of rows of identical elements of length $2l$. Each dipole is loaded with the same impedance Z_L. Each row has $2K+1$ number of identical elements spaced at a distance D_x apart. The distance between two adjacent rows is D_Z.

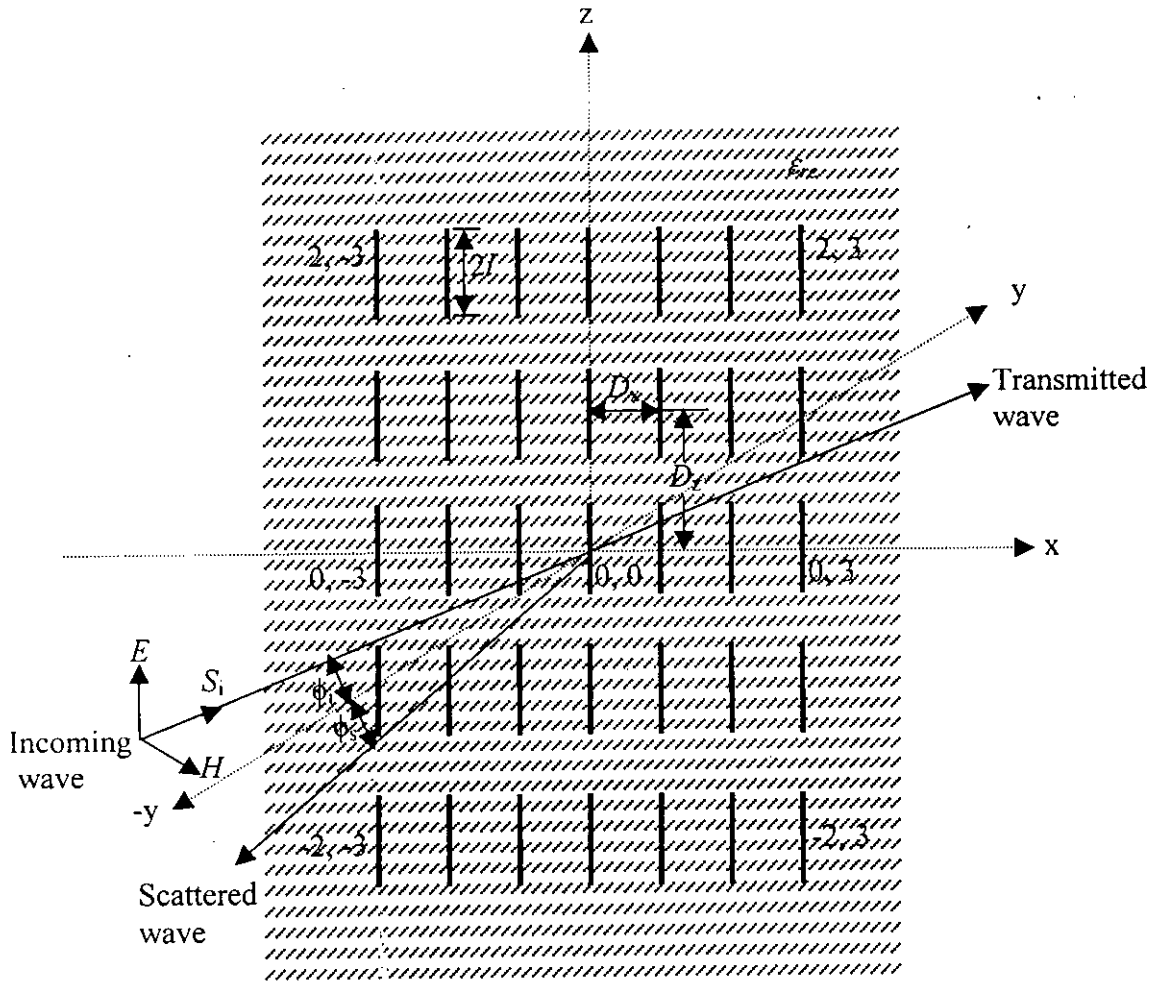

Fig.3.3 Array of loaded dipoles in a homogeneous dielectric medium (ε_{re}) and incident EM wave with vertical polarization.

The mutual impedance, $Z_{r'k}$ of this array can be expressed as

$$Z_{r'k} = \frac{j\beta}{8\pi\omega\varepsilon} \int_{r'D_z - l}^{r'D_z + l} \left[\sin\beta z \int_{-l}^{+l} \frac{\partial}{\partial z} \left(\frac{\exp\{-j\beta(z_1 + r)\} + \exp\{j\beta(z_1 - r)\}}{r} \right) dz_1 \right] dz$$

$$-\frac{\omega\mu}{8\pi} \int_{r'D_z - l}^{r'D_z + l} \left[\sin\beta z \int_{-l}^{+l} \left(\frac{\exp\{-j\beta(z_1 + r)\} - \exp\{j\beta(z_1 - r)\}}{r} \right) dz_1 \right] dz \quad (3.18)$$

where $r = [\,(k D_x)^2 + (z - z_1)^2\,]^{1/2}$

z_1 = z coordinate on the dipole.

r' = number of rows which varies from $-R''$ to R''.

k = number of columns which varies from -K to K.

For easier and more accurate numerical computation, eqn. 3.18 can be rewritten introducing effective length of the dipole as follow [12].

$$Z_{r'k} = \frac{j\beta}{8\pi\omega\varepsilon} \int_{r'D_z + l}^{r'D_z - l} \left[\sin\beta\left(l_e - |z|\right) \int_{l}^{-l} \frac{\partial}{\partial z} \left(\frac{\exp\{-j\beta(\Delta z' + r)\} + \exp\{j\beta(\Delta z' - r)\}}{r} \right) dz_1 \right] dz$$

$$-\frac{\omega\mu}{8\pi} \int_{r'D_z + l}^{r'D_z - l} \left[\sin\beta\left(l_e - |z|\right) \int_{l}^{-l} \left(\frac{\exp\{-j\beta(\Delta z' + r)\} - \exp\{j\beta(\Delta z' - r)\}}{r} \right) dz_1 \right] dz \quad (3.19)$$

where $\Delta z' = l_e - |z_1|$

$2l_e$= effective length of each dipole.

Eqn. 3.19 is applicable only for the array of dipole antennas whose lengths are the odd multiples of the half-wave length as mentioned in section 3.2.1. The mutual impedance of the array consists of dipoles of any length can be written as [27].

$$Z_{r'k} =$$

$$\frac{j\beta}{8\pi\omega\varepsilon \sin^2 \beta l_e} \int_{r'D_z - l}^{r'D_z + l} \left[\sin\beta\left(l_e - |z|\right) \int_{l}^{-l} \frac{\partial}{\partial z} \left(\frac{\exp\left\{-j\beta\left(\Delta z' + r\right)\right\} + \exp\left\{j\beta\left(\Delta z' - r\right)\right\}}{r} \right) dz_1 \right] dz$$

$$-\frac{\omega\mu}{8\pi \sin^2 \beta l_e} \int_{r'D_z - l}^{r'D_z + l} \left[\sin\beta\left(l_e - |z|\right) \int_{l}^{-l} \left(\frac{\exp\left\{-j\beta\left(\Delta z' + r\right)\right\} - \exp\left\{j\beta\left(\Delta z' - r\right)\right\}}{r} \right) dz_1 \right] dz \qquad (3.20)$$

The reflection coefficient of the array can then be obtained by using eqn. 3.20.

3.4 SE OF THE ARRAY OF DIPOLES

SE consists of absorption loss (A), reflection loss (R) and successive reflection loss (B) of the RFCP. For a doubly periodic array of dipoles in an equivalent homogeneous medium (ε_{re}) as shown in Fig. 3.3, there will be no absorption loss due to the use of strip like filler. Successive reflection loss is very negligible. SE of the array of dipoles in a homogeneous medium having an effective dielectric constant (ε_{re}) can then be expressed as follow

$$\text{SE} = R \quad \text{dB} \qquad (3.21)$$

Reflection loss (R) can be determined by multiplying the incident power with the reflection coefficient (R^I).

3.4.1 Reflection coefficient of the array of dipoles

A plane wave, which is incident on the periodic array of dipoles as shown in Fig. 3.3 is considered to be linearly polarized in z direction. The direction of propagation lies in the x-y plane, making an angle ϕ_i with negative y-axis as shown in Fig.3.3. Detailed derivation of the reflection coefficient is given in Appendix A. The specular reflection coefficient for such an array (i.e. FSS) can be expressed as [15].

$$R^I = \frac{K(l_\lambda, l_e, Z_L, Z_A)\, l^4 \sec^2 \phi_i}{[D_x D_z (Z_i + Z_l)]^2} \tag{3.22}$$

where $$K(l_\lambda, l_e, Z_L, Z_A) = 3600 \frac{\left| F_{e1} - \left(\frac{Z_L}{Z_A}\right) F_{e2} \right|^2 F_{e3}^{\,2}}{\pi^2 l_\lambda^{\,4}}$$

$$F_{e1} = \frac{\sin \beta l - \beta l_e \cos \beta l_e}{1 - \cos \beta l_e}$$

$$F_{e2} = \frac{1}{\sin \beta l_e} \left[1 - \cos \beta l_e - F_{e1} \sin \beta l_e \right]$$

and $$F_{e3} = \frac{\cos \beta\, \Delta l - \cos \beta\, l_e}{\sin \beta\, l_e}$$

In the above equations, $l_\lambda = l/\lambda$, where λ is the wavelength of the incident wave, $\Delta l = l_e - l$, $\beta = 2\pi/\lambda$ is the phase constant and Z_A is the driving point impedance of each element.

The driving point impedance of the array can be written as [15].

$$Z_A = \sum_{r'=-R''}^{R''} \sum_{k=-K}^{K} \varepsilon_k \, Z_{r'k} \cos(\beta \, D_x \, k \sin\phi_i) \qquad (3.23)$$

where ε_k is the Neumann factor defined by

$$\varepsilon_k = 1 \qquad \text{for } k = 0$$

$$= 2 \qquad \text{for } k \neq 0$$

3.5 SE OF THE ARRAY OF SMALL SQUARE LOOPS

For the array of small square loops in a homogeneous medium having an effective dielectric constant (ε_{re}), reflection loss (R) as well as absorption loss (A) will be available. There will be no successive reflection loss (B) due to the use of thin square loop like filler. SE of such RFCP can be expressed as

$$\text{SE} = A + R \qquad \text{dB} \qquad (3.24)$$

where A is the absorption loss and R is the reflection loss. Reflection coefficient and absorption loss has been evaluated in the following subsections.

3.5.1 Reflection coefficient of the array of small square loops

A doubly periodic array of small square loops in a homogeneous medium having an effective dielectric constant (ε_{re}) is shown in Fig.3.4.

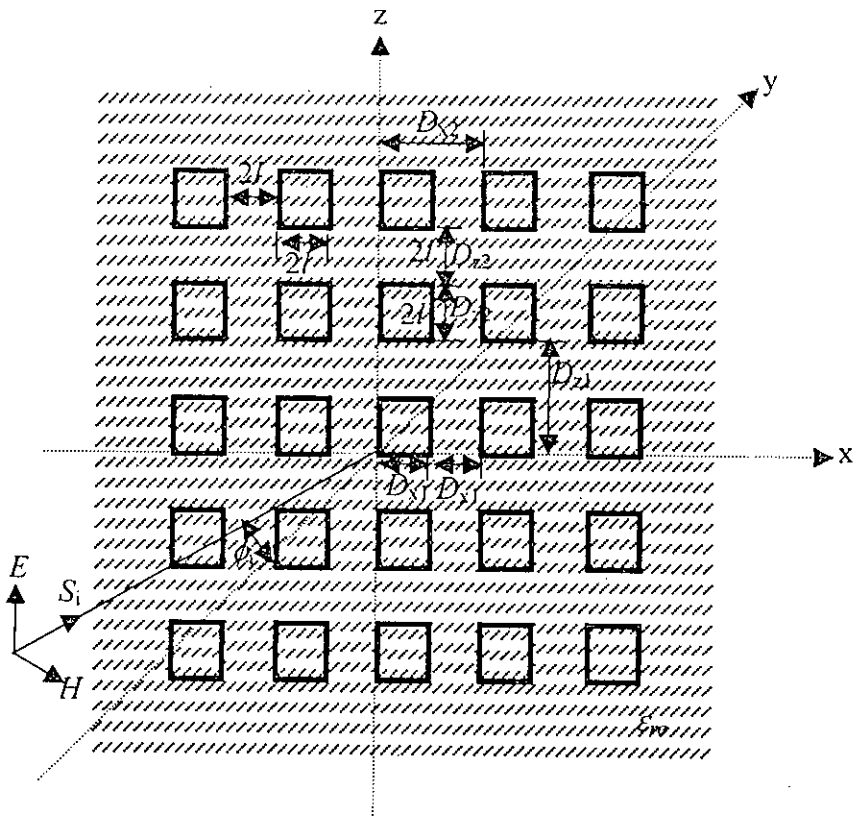

Fig. 3.4 Array of square loops in a homogeneous dielectric medium (ε_{re}).

In this case for computing the reflection coefficient, this type of array configuration has been considered as a combination of vertical (z-directed) array and horizontal (x-directed) array of dipoles by satisfying the following conditions.

- number of rows and number of columns of the vertical and horizontal dipole array must be even and equal i.e. $r_1' = r_2' = r'$ and $k_1 = k_2 = k$.

- length of element for both the vertical and horizontal arrays must be equal and should be electrically small.

- spacing between two adjacent array element in the case of vertical array (i.e. z-directed) will be as follow: $D_{x1} = 2l$ and $D_{z1} = 2D_{z2} = 4l$

- spacing between two adjacent array element in the case of horizontal array (x-directed) will be as follow: $D_{x2} = 2D_{x1} = 4l$ and $D_{z2} = 2l$

The reflection coefficient of the array of small square loops as shown in Fig.3.4 will then be

$$R' = R'_1 + R'_2 \tag{3.25}$$

where R'_1 is the reflection coefficient of the vertical array of dipoles and R'_2 is the reflection coefficient of the horizontal array of dipoles. Derivations of R'_1 and R'_2 are given in the following subsections.

In the case of square loop there will be no free charge on the loop i.e. $\rho_l = 0$ [28]. Thus the scalar potential term of eqn. 3.9 will be zero. The electric field will then be only due to the vector potential. The electric field eqn. (3.15) becomes as

$$E_z = \frac{\omega\mu I_1}{8\pi} \int_{-l}^{+l} \left(\frac{e^{-j\beta(z_1+r)} - e^{j\beta(z_1-r)}}{r} \right) dz_1 \tag{3.26}$$

3.5.1.1 Reflection coefficient of vertical array

Reflection coefficient of vertical array (i.e. z directed dipoles) as described in section 3.5.1 is determined in a similar manner as that of the array of z directed dipoles. The mutual impedance of the vertical array can be expressed as

$$Z_{1r'k} =$$

$$-\frac{\omega\mu}{8\pi \sin^2 \beta l_e} \int_{r'D_{z1}}^{r'D_{z1}+2l} \left[\sin \beta\left(l_e - |z|\right) \int_0^{2l} \left(\frac{\exp\left\{-j\beta\left(\Delta z' + r_1\right)\right\} - \exp\left\{j\beta\left(\Delta z' - r_1\right)\right\}}{r_1} \right) dz_1 \right] dz \tag{3.27}$$

where $r_1 = [\,(kD_{x1})^2 + (z-z_1)^2\,]^{1/2}$

z_1 = z coordinate on the dipole

$\Delta z' = l_e - |z_1|$

r' = number of rows which varies from $-R''$ to $(R''+1)$.

k = number of columns which varies from $-K$ to $(K+1)$.

Driving point impedance of vertical array is determined as

$$Z_{1A} = \sum_{r'=-R''}^{R''+1} \sum_{k=-K}^{K+1} \varepsilon_k \; Z_{1r'k} \cos(\beta \, D_{x1} \, k \sin\phi_i) \tag{3.28}$$

Reflection coefficient of the vertical array then yields as

$$R_1' = \frac{K_1(l_\lambda, l_e, Z_L, Z_{1A})\, l^4 \sec^2\phi_i}{[D_{x1} D_{z1} (Z_{1A} + Z_L)]^2} \tag{3.29}$$

where $$K_1(l_\lambda, l_e, Z_L, Z_{1A}) = 3600 \frac{\left| F_{e1} - \left(\frac{Z_L}{Z_{1A}}\right) F_{e2} \right|^2 F_{e3}^{\,2}}{\pi^2 l_\lambda^{\,4}}$$

F_{e1}, F_{e2}, F_{e3} are as given in section 3.4.1.

3.5.1.2 Reflection coefficient of the horizontal array

Reflection coefficient of the horizontal array (i.e. x-directed dipoles) as mentioned in section 3.5.1 is determined in a similar way to that of the vertical array. The mutual impedance of the horizontal array can be expressed as

$$Z_{2r'k} =$$

$$-\frac{\omega\mu}{8\pi \sin^2 \beta l_e} \int_{r'D_{x2}}^{r'D_{x2}+2l} \left[\sin\beta\left(l_e - |x|\right) \int_0^{2l} \left(\frac{\exp\left\{-j\beta\left(\Delta x' + r_2\right)\right\} - \exp\left\{j\beta\left(\Delta x' - r_2\right)\right\}}{r_2} \right) dx_1 \right] dx \tag{3.30}$$

where $r_2 = [\,(kD_{z2})^2 + (x-x_1)^2\,]^{1/2}$

x_1 = x coordinate on the dipole

$\Delta x' = l_e - |\,x_1\,|$

Driving point impedance of horizontal array yields as

$$Z_{2A} = \sum_{r'=-R''}^{R''+1} \sum_{k=-K}^{K+1} \varepsilon_k \, Z_{2r'k} \cos(\beta\, D_{z2}\, k \cos\phi_i) \tag{3.31}$$

Reflection coefficient of the horizontal array then becomes as

$$R_2' = \frac{K_2\,(l_\lambda, l_e, Z_L, Z_{2A})\, l^4 \operatorname{cosec}^2\phi_i}{[D_{x2} D_{z2}\left(Z_{2A} + Z_L\right)]^2} \tag{3.32}$$

where $$K_2(l_\lambda, l_e, Z_L, Z_{2A}) = 3600 \frac{\left| F_{e1} - \left(\frac{Z_L}{Z_{2A}}\right) F_{e2} \right|^2 F_{e3}^2}{\pi^2 l_\lambda^4}$$

3.5.2 Absorption loss of the array of small square loops

Voltage induced in the loop due to the incident field can be expressed as follow [3].

$$V_{11} = \frac{1}{I_1} \int_0^{2l} I_z E_z \, dz \tag{3.33}$$

Substituting eqn. 3.1 and eqn. 3.26 into eqn. 3.33 yields

$$V_{11} = \frac{\omega\mu}{8\pi} \int_0^{2l} \left[\sin \beta z \int_0^{2l} \left(\frac{e^{-j\beta(z_1+r)} - e^{j\beta(z_1-r)}}{r} \right) dz_1 \right] dz \tag{3.34}$$

Eqn. 3.34 is restricted for the case where each side of the square loop is equal to the odd multiple of the half wavelength. For the case of the loop sides of any length eqn. 3.34 becomes

$$V_{11} = \frac{\omega\mu}{8\pi \sin^2 \beta l_e} \int_0^{2l} \left[\sin \beta z \int_0^{2l} \left(\frac{e^{-j\beta(z_1+r)} - e^{j\beta(z_1-r)}}{r} \right) dz_1 \right] dz \tag{3.35}$$

By small loop approximation (i.e. loop perimeter << λ), loop loss resistance is found as follow [3]

$$R_L = \frac{L}{2a} \sqrt{\frac{f \mu_0}{\pi \sigma}} \tag{3.36}$$

where L = loop perimeter, m

a = wire (conductor or dipole) radius, m

σ = conductivity of the loop material , mhos/m

Absorption loss in a loop will then be as

$$A_L = \frac{V_{11}^{\ 2}}{R_L} \tag{3.37}$$

Total absorption loss (dB) in the array of small square is then obtained as

$$A = 10\log_{10}\left(A_L M\right) \quad dB \tag{3.38}$$

where M is the total number of loops in the array.

CHAPTER 4

RESULTS AND DISCUSSIONS

- INTRODUCTION
- REFLECTION COEFFICIENT AT VARIOUS FREQUENCIES
- EFFECT OF INCIDENCE ANGLE
- EFFECT OF RFCP GEOMETRIES
- EFFECT OF DIELECTRIC SUBSTRATE
- REFLECTION COEFFICIENT OF STRIP ARRAY AND SQUARE LOOP ARRAY
- ABSORPTION LOSS OF THE SQUARE LOOP ARRAY

4.1 INTRODUCTION

The reflection coefficient of the RFCP containing both strip like filler and square loop type filler has been computed in the frequency range of 1 GHz to 12 GHz. Reflection coefficient depends on substrate type, number of filler on the substrate, filler length, spacing between two adjacent fillers and incidence angle. SE value of the RFCP containing the small square loop like filler is due to the reflection loss and absorption loss. A comparison between the reflection coefficient of RFCP containing strip like filler with that of containing the square loop like filler which perimeter is equal to the strip length is given in this chapter. Absorption loss of the RFCP containing the square loop like filler is also computed in this chapter. Through out the computation of reflection coefficient, no loading (i.e. $Z_L = 0$) is considered for simplicity.

4.2 REFLECTION COEFFICIENT AT VARIOUS FREQUENCIES

The reflection coefficient of the array of strip like fillers (RFCP) on a dielectric substrate is computed at various frequencies. The geometrical data of the RFCP on the substrate are: filler length ($2l$) = 4 cm, horizontal spacing between two adjacent fillers (D_x) = 2 cm, vertical spacing between two adjacent fillers (D_z) = 5 cm and substrate thickness (h) = 0.1 cm. Polyvinyl Chloride is considered as a substrate which dielectric constant is 4.5. The number of fillers on the substrate is taken as 25 and normal incidence of the field is considered. A plot of the reflection coefficient as a function of frequency is shown in Fig. 4.1. The angle of reflection coefficient as a function of frequency is given in Appendix B.

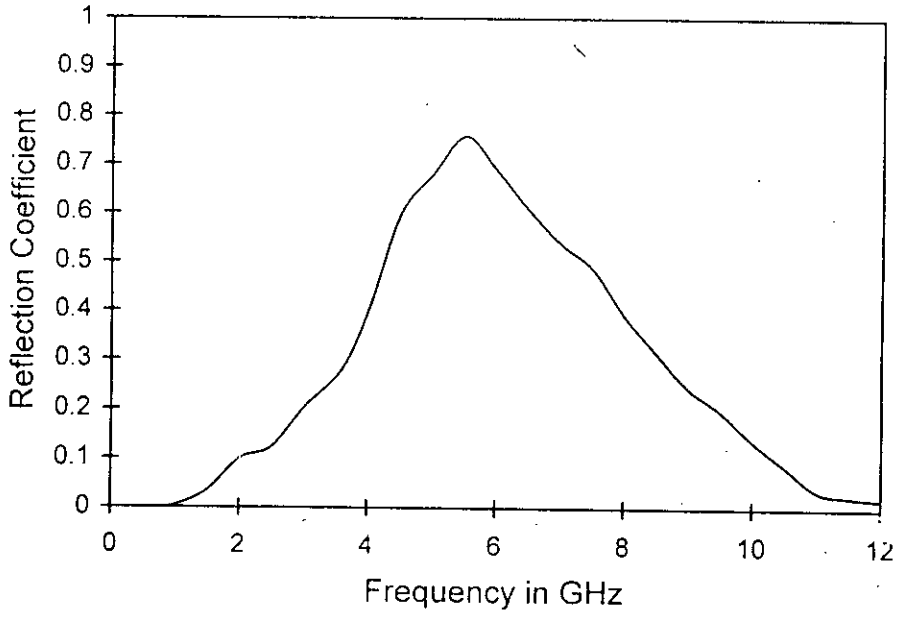

Fig. 4.1 Reflection coefficient as a function of frequency.

The Fig. 4.1 shows that the reflection coefficient below frequency 2 GHz and above frequency 11 GHz is very negligible. It is also observed from Fig. 4.1 that the magnitude of the reflection coefficient increases as the frequency increases first and attains a peak value of about 0.76 at a frequency of 5.5 GHz which may be due to the resonance at that frequency. After resonance, the reflection coefficient decreases, which is expected [12]. Fig. 4.1 shows that the reflectivity of the array of strip like filler on a dielectric substrate is largely dependent on the frequency of the incident field. It can be noted here that this type of RFCP can be used for a certain range of frequency where reflection coefficient is significant.

4.3 EFFECT OF INCIDENCE ANGLE

Reflection coefficient of the same RFCP as mentioned in section 4.2 is computed for different incidence angle. A set of curves of the reflection coefficient for different incidence angles is shown in Fig. 4.2.

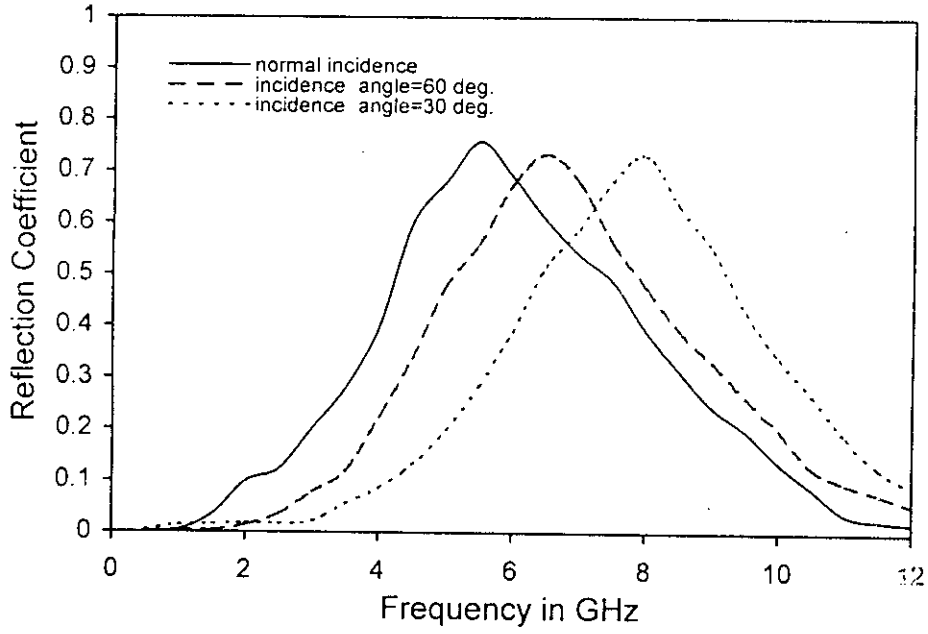

Fig. 4.2 Reflection coefficients for various incidence angles.

The Fig. 4.2 shows that the maximum reflection due to the change of incidence angles remain unchanged. This may be due to the occurring of reflection from the same RFCP (i.e. same FSS). However the maximum reflection is occurred at different resonance frequencies because of considerable effect on the driving point impedance due to the change in incidence angle. This exhibits the properties of FSS [15].

4.4 EFFECT OF RFCP GEOMETRES

Reflection coefficient depends on RFCP geometries such as length of the filler ($2l$), horizontal spacing (D_x) and vertical spacing (D_z) between two adjacent fillers and number of filler on the substrate. Effects on reflection coefficient due to the change of RFCP geometries are described in the following subsections.

4.4.1 Effect of horizontal spacing

The reflection coefficient is computed for different horizontal spacing between two adjacent fillers of the RFCP. The same RFCP as mentioned in section 4.2 is taken and normal incidence is considered to compute the reflection coefficient. Reflection coefficients for different horizontal spacings (D_x) are shown in Fig. 4.3.

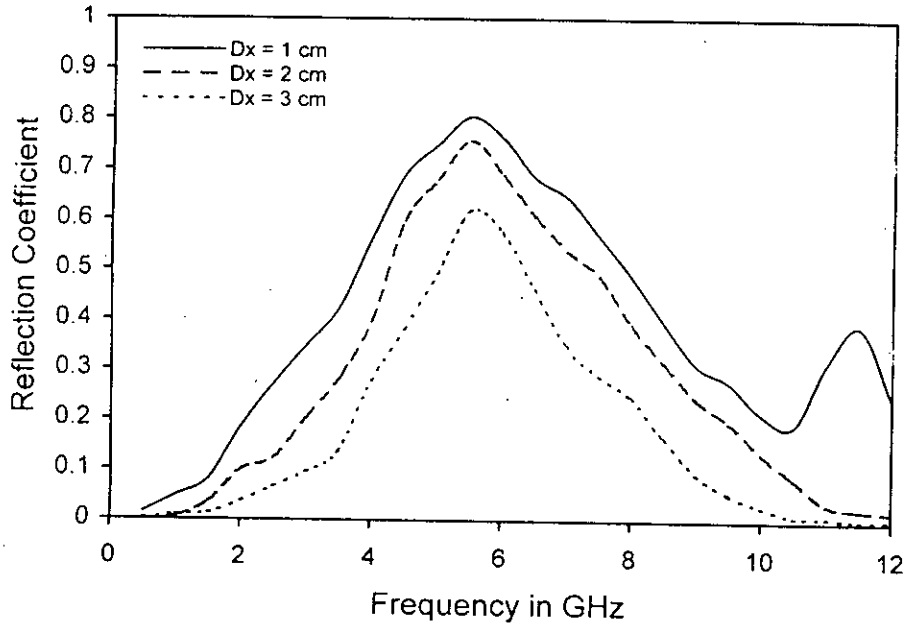

Fig.4.3 Reflection coefficients for different horizontal spacing.

The Fig.4.3 shows that as the horizontal spacing between two adjacent fillers reduces (i.e. the filler density of the RFCP increases), the reflection increases. This is due to the square of inverse proportionality of the horizontal spacing between two adjacent fillers (D_x) and the reflection coefficient. Again driving point impedance is a function of horizontal spacing (refers to eqn. 3.20). Thus the change in reflection coefficient due to change in horizontal spacing between two adjacent fillers is obvious. It is also observed from Fig. 4.3 that as the horizontal spacing

increases the band of frequency for which reflection is significant is reduced, whereas resonance is found at the same frequency. For a RFCP of very closely arranged fillers (e.g. D_x = 1 cm, refers to Fig 4.3) the resonance may be occurred at different frequencies.

4.4.2 Effect of vertical spacing

The reflection coefficient is also computed for different vertical spacing between two adjacent fillers (D_z) of the same RFCP geometries as mentioned in section 4.2. Reflection coefficients for different vertical spacing between two adjacent fillers are shown in Fig. 4.4.

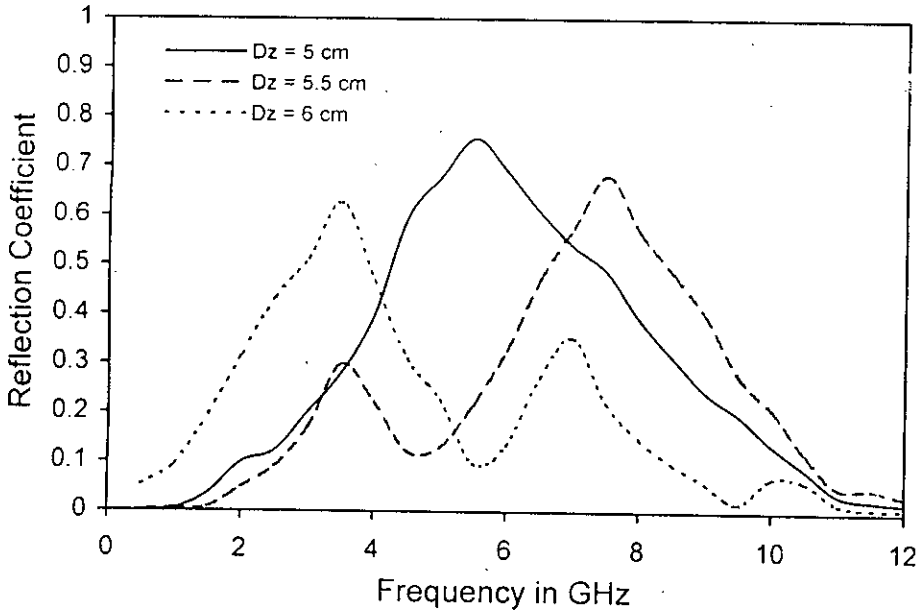

Fig.4.4 Reflection coefficients for different vertical spacing.

Fig. 4.4 shows that with increasing of the vertical spacing between two adjacent fillers, the reflection decreases. It is expected from eqn. 3.22. Fig. 4.4 also shows that for different vertical

spacing between two adjacent fillers (D_z), resonances are occurred at different frequencies. This may be due to the vertical polarization (i.e. z-directed E field) as well as the dependency of the mutual impedance on the vertical separation between two adjacent fillers.

4.4.3 Effect of number of fillers

The reflection coefficient of the array of dipole like fillers on a dielectric substrate (RFCP) for different number of fillers is computed. Same RFCP geometries as described in section 4.2 are taken for computation and normal incidence is considered. Reflection coefficients for two different numbers of filler elements (225 and 25 filler elements) are shown in Fig. 4.5.

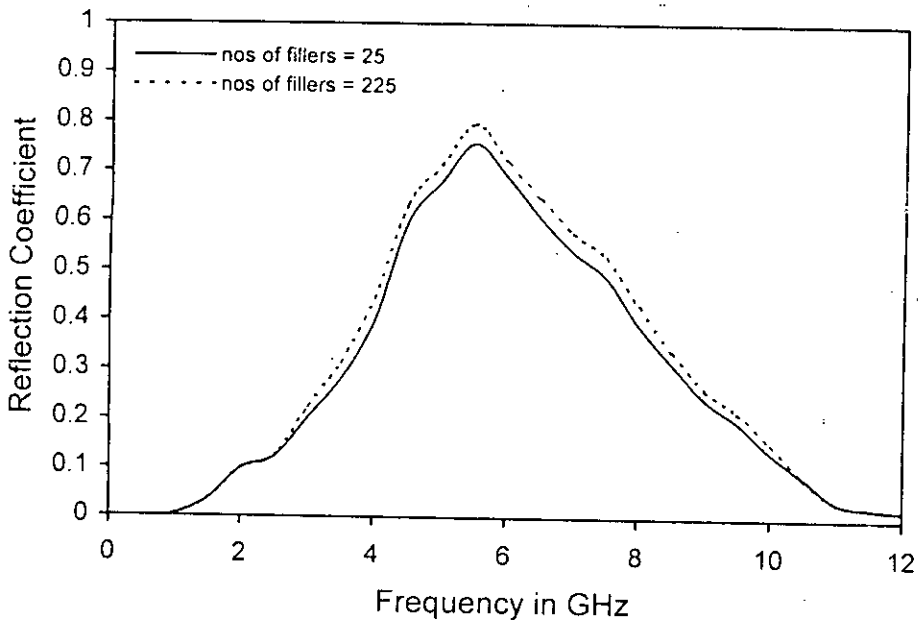

Fig.4.5 Reflection coefficients for different number of fillers.

The Fig.4.5 shows that the array consists of 25 element gives lower reflectivity. One probable reason for this lower reflectivity is that in the analysis of driving point impedance it was assumed

that the array is very large and as such the driving point impedance of the central element (Z_{00}) can be repeated for all the filler elements in the array.

4.5 EFFECT OF DIELECTRIC SUBSTRATE

Reflection coefficient also depends on the dielectric constant (ε_r) of the used substrate material as well as substrate thickness (h). Effects of dielectric constant of the substrate and substrate thickness on reflection coefficient are described in the following subsections.

4.5.1 Effect of dielectric constant

The reflection coefficient of the array of dipole like filler for free standing condition (i.e. dipole array in free space) is computed. Computation is then repeated in the case of the RFCP on a dielectric substrate having dielectric constant 4.5. The comparison between the two computed reflection coefficients is shown in Fig. 4.6.

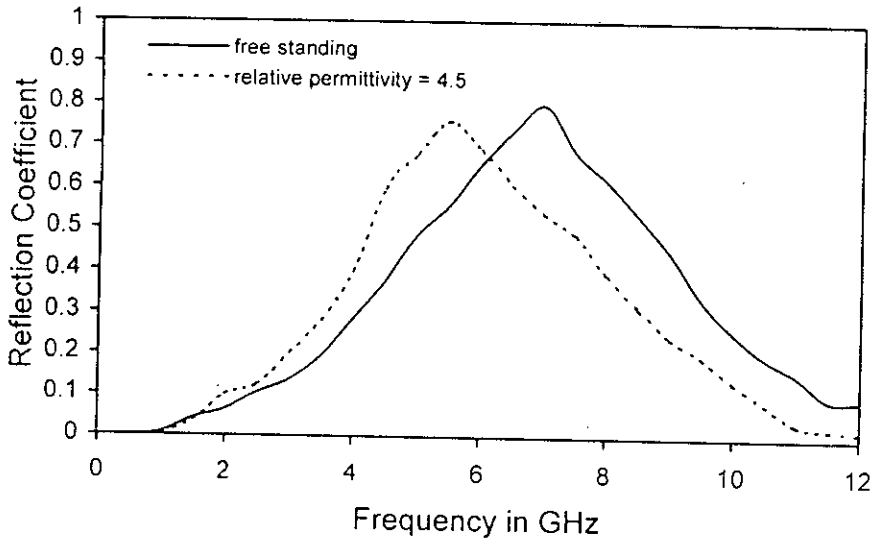

Fig.4.6 Reflection coefficients of FSS for free standing condition and on a dielectric.

Normal incidence of the field is considered and the same geometries of the array as described in section 4.2 are chosen for the analysis.

It is evident from Fig.4.6 that the reflection coefficient of FSS for free standing condition is higher than that of the FSS on dielectric substrate such as polyvinyl chloride. This may be due to the existence of more electric field in the substrate than that of the air. Fig.4.6 also shows that the band of frequency for significant reflection is found at a higher frequency region for free standing condition than that of the FSS on polyvinyl chloride. This may be due to the change of mutual impedance because of dielectric substrate. Making a shielded enclosure for electronic equipment to fight against EMI is the main objective for developing this type of composite plastic. In making such a shielded enclosure, different dielectric materials can be used as substrate. A list of commonly used plastic substrate materials is given in Appendix C.

The effects of types of substrates on reflection coefficient of the array of dipole like filler (RFCP) are also observed in this work. The same RFCP geometries as stated in section 4.2 are considered. Polyethylene, quartz and polyvinyl chloride are taken as dielectric substrate having a relative dielectric constant of 2.5, 3.8 and 4.5 respectively. Normal incidence of the field is considered. Reflection coefficients of the RFCP for the case of different types of substrates are illustrated in Fig. 4.7.

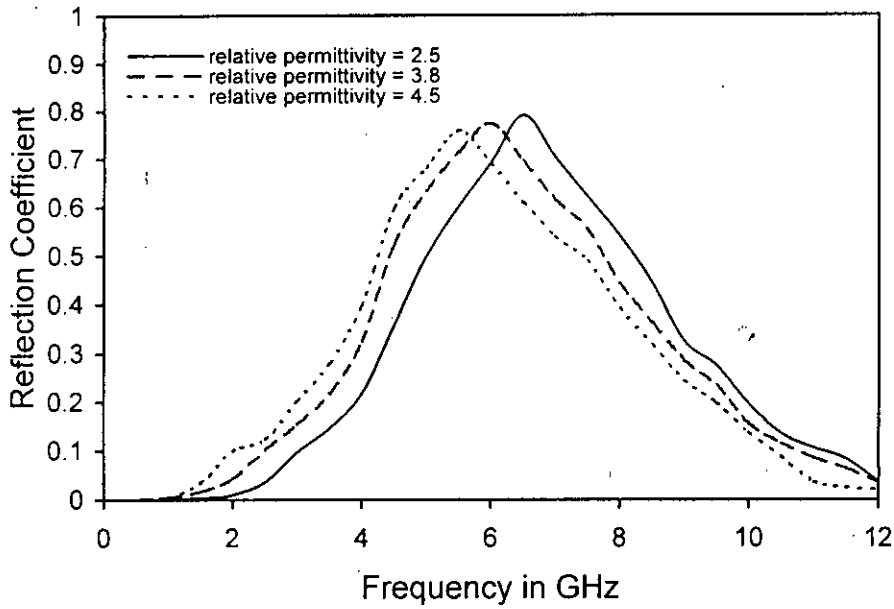

Fig.4.7 Reflection coefficients for different dielectric substrates.

Fig.4.7 shows that as the dielectric constant of the substrate increases, the reflection from the RFCP decreases. It is also evident from Fig.4.7 that the frequency band for significant reflection is shifted to a lower frequency region with the increase of ε_r. This may be due to the change in mutual impedance with change in the substrate permittivity (refers to eqn. 3.20) and the characteristic of dielectric material of conserving more electric field than that of air (refers to Fig. 2.8). The relationship between resonant frequency and relative permittivity is given in Appendix D.

4.5.2 Effect of substrate thickness

Reflection coefficient of the array of dipole like filler on a dielectric substrate (RFCP) is computed for different substrate thickness (h). The same geometrical data of the RFCP as mentioned in section 4.2 are considered. Reflection coefficient is computed for normal

incidence. A set of curves of reflection coefficient for different substrate thickness (h) is shown in Fig. 4.8.

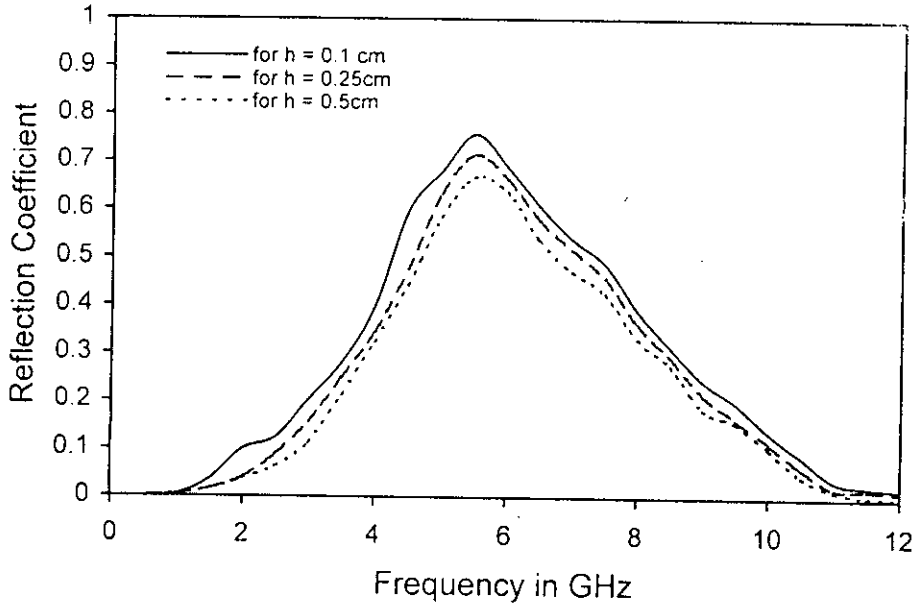

Fig.4.8 Reflection coefficients for different substrate thickness.

It is observed from Fig.4.8 that as the substrate thickness (h) increases the reflection from the RFCP decreases. This may be due to the fact that a thicker substrate conserves more electric field than that of a thinner one. Practically thin substrate is desirable because of many advantages such as less material requirement, low cost, lightweight and easy formability. It is also evident from Fig.4.8 that RFCP on thin substrate exhibits better reflectivity which, results in better shielding effectiveness (SE) of the RFCP. Thus it can be recommended to use the RFCP on a thin substrate for making the shielded enclosure for electronic equipment.

4.6 REFLECTION COEFFICIENT OF STRIP ARRAY AND SQUARE LOOP ARRAY

Reflection coefficient is computed for the array of dipole like fillers and the array of square loop like fillers. The geometrical data of array of dipole like fillers are: filler length ($2l$) = 4 cm, horizontal spacing between two adjacent fillers (D_x) = 0.8 cm, vertical spacing between two adjacent fillers (D_z) = 5 cm and substrate thickness (h) = 0.1 cm. Polyvinyl Chloride is considered as the substrate material in both cases. The number of fillers on the substrate is taken as 25 and normal incidence of the field is considered. In case of computing reflection coefficient of the array of square loop like fillers following geometries are considered: loop perimeter = 4 cm (i.e. loop perimeter is equal to the length of the strip), number of loops = number of strips, distance between two adjacent loops = 1 cm. The comparison between the reflection coefficient of RFCP with strip like fillers and that of the RFCP with loop like fillers is shown in Fig. 4.9.

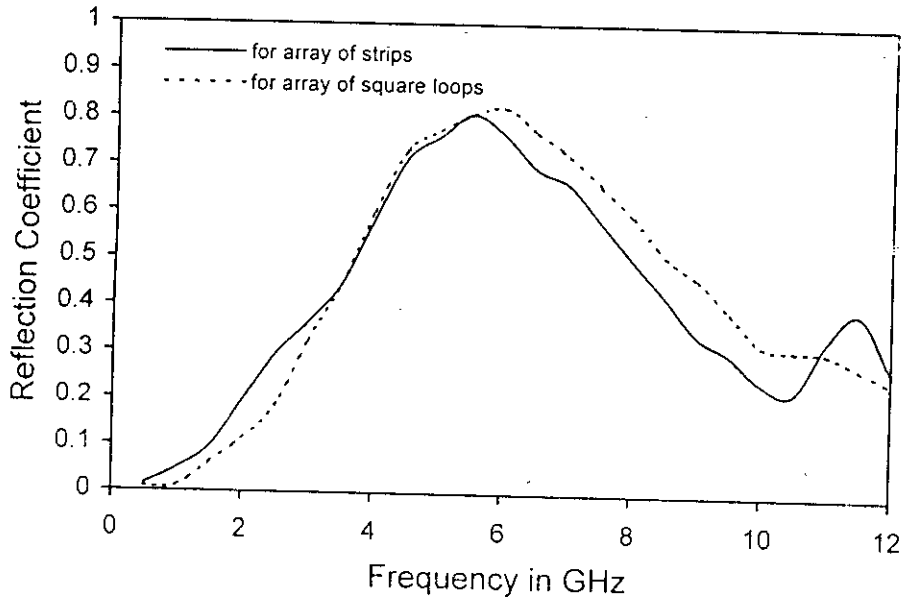

Fig.4.9 Reflection coefficients of strip array and square loop array.

To compare the reflection coefficient of the array of strips and the array of square loops, same surface area (100 sq. cm) and thickness (0.1 cm) of the substrate are considered. The perimeter of each loop is equal to the length (*2l*) of each strip and the number of loops equal to the number of strips. So same amount of conducting material (copper) is used for both computations. It is evident from Fig. 4.9 that reflection from square loop array is smaller than that of the strip array below frequency 3.5 GHz. As the frequency increases the reflection from the square loop array becomes greater than that of the strip array up to frequency 11 GHz. Beyond this frequency reflection from the array of square loops becomes smaller. So, for a frequency band of 3.5 GHz-11GHz, the reflection coefficient is greater for the square loop array than that of the strip array.

4.7 ABSORPTION LOSS OF THE SQUARE LOOP ARRAY

Absorption loss of the array of square loops is also computed from the loop resistive loss. The same geometrical data of the square loop array as described in section 4.6 are considered. Copper is taken as conducting material which conductivity (σ) is 5.8×10^7 mhos/meter. Normal incidence of the field is considered. The computed absorption loss (*dB*) as a function of frequency is shown in Fig. 4.10.

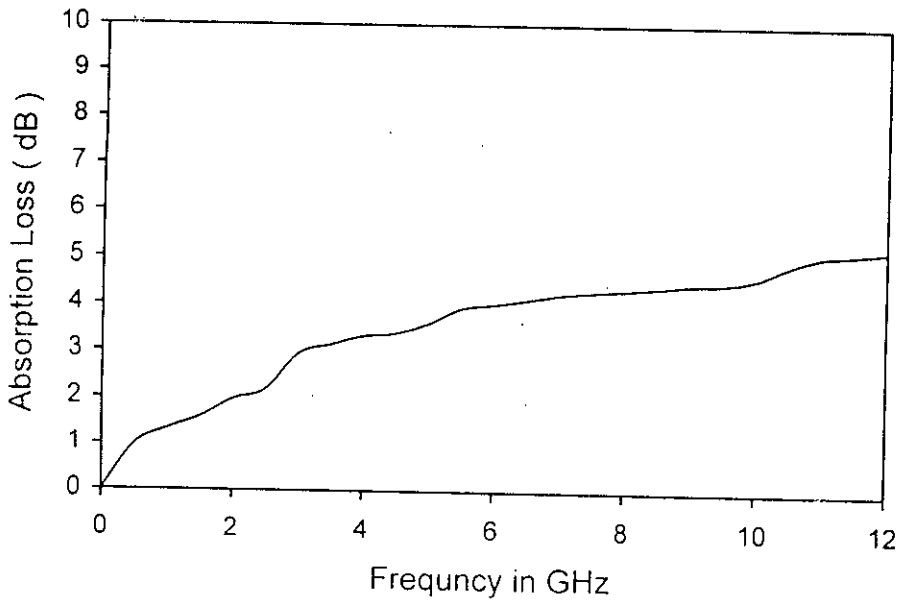

Fig.4.10 Absorption loss of the square loop array.

Fig. 4.10 shows that the absorption loss in the array of square loop like fillers increases with frequency. Loss resistance of the loop increases with frequency (refers to eqn.3.3). Induced voltage in the loop is also a function of frequency (refers to eqn.3.35). Thus computed absorption loss in the loop array increases with frequency and it is expected.

SE of the RFCP of square loop like fillers depend on reflection loss and absorption loss (refers to section 2.2). In section 4.6 it is shown that for a frequency band (3.5 GHz-11GHz) the reflection of square loop array is better than that of strip array considering same area to be shielded and same amount of conducting and substrate materials used. Absorption loss is also present in this type of RFCP which is shown in Fig.4.10. SE of the strip array depends on refection loss only (refers to section 2.2). Thus SE of the RFCP of square loop like fillers is better than that of the RFCP of strip like fillers.

CHAPTER 5

CONCLUSION AND RECOMMENDATIONS FOR FUTURE WORK

- CONCLUSION
- RECOMMENDATIONS FOR FUTURE WORK

5.1 CONCLUSION

Evaluation of the shielding effectiveness (SE) of a regularly filled conductive composite (RFCP) for electromagnetic shielding was the main objective of this research. Two types of fillers (i.e. strip like filler and square loop like filler) in a plastic resin has been proposed to produce a RFCP as a shielding material. These types of RFCP can be used in making enclosure for various types of electronic equipment to combat against electromagnetic interference (EMI) and electrostatic discharge (ESD).

Some important features of FSS along with the related theoretical background have been described in this thesis for better understanding of the salient features of the developed RFCP (FSS). Mathematical model for determining shielding effectiveness of the RFCP with strip like filler has been developed in terms of reflection coefficient. Reflection coefficient is then determined by a series of computer program written in C^{++} language, which is run in Pentium machine. Reflection coefficient has also been derived for RFCP with square loop like filler. Absorption loss, which is found in RFCP containing loop like filler is also derived analytically. Absorption loss is then computed by a series of program written in C^{++} language. The computer programs are given in Appendix E. Throughout the computation no loading (i.e. Z_L=0) is considered for simplicity. This is also due to the fact that during making the shielded enclosure for electronic equipment no loading condition has to be considered.

It has been observed that significant reflection from the RFCP can be achieved for a specific band of frequencies (refers to section 4.2 and 4.6). The attenuation of EM waves due to the reflection from conductive fillers of such types of RFCP has been studied theoretically. Experimental investigation has not been carried out due to the unavailability of test equipment and related facilities.

The resonant frequency of the array as well as the bandwidth depends strongly on the strip (dipole) element. Resonant frequency and bandwidth is also influenced by the RFCP geometries, angle incidence of the field and substrate material.

It is observed that RFCP of square loop like filler exhibits better reflectivity than that of strip like filler (refers to Fig.4.9). More over, absorption loss has been found in square loop array (refers to Fig.4.10). Thus it can be concluded that the RFCP consisting the square loop like filler has better shielding capability than that of the strip like filler.

One notable features of the regularly filled conductive composite (both of strip like filler and square loop like filler) is that the shielding capability which can be controlled by proper selection of the shape, size and separation between two adjacent fillers. Moreover SE values can also be predicted prior to manufacturing which is not possible in the case of available randomly filled conductive composites.

5.2 RECOMMENDATIONS FOR FUTURE WORK

The following recommendations are made to carry out the future research.

- Due to the unavailability of the necessary instruments, it was not possible to measure the SE of the RFCP. Thus measurement of the SE of the RFCP could be carried out to compare the predicted SE value with the measured SE value.

- In this work the RFCP (FSS) element are attached to the surface of the substrate. On the other hand during the moulding process of the filled composite material, filler will be embedded in the plastic resin. This configuration is very similar to a material where the

fillers would be sandwiched between two types of dielectric materials. Thus more rigorous analysis is required to find the SE of such type of RFCP.

- Evaluation of shielding effectiveness of FSS like RFCP from reflection coefficient is not carried out by other techniques as mentioned in the introducing chapter. This was beyond the scope of this work. Thus it was not possible to find the computational accuracy of the proposed technique. Evaluation of shielding effectiveness of RFCP from reflection coefficient by any other techniques such spectral domain technique can be an interesting topic for further research. The computational accuracy of the presented technique can then be found by comparing the reflection coefficient obtained from the other techniques.

- In finding the reflection coefficient and absorption loss of the square loop array, small loop approximation is considered. The SE could be find out for the array of loops of any shape (i.e. triangular, circular, rectangular) and size. A rigorous analysis is required to find the SE value of the RFCP containing the array of loops of any size. This analysis could be carried out in future by the same technique or by any other technique, which has been mentioned in the introductory chapter of this thesis.

APPENDICES

REFLECTION COEFFICIENT OF THE ARRAY OF LOADED DIPOLES IN A HOMOGENEOUS DIELECTRIC MEDIUM [15].

The periodic passive array shown in Fig.3.3 is considered. An incidence plane wave has a power density S_i and is polarized in z direction is considered also. The direction of propagation lies in the x-y plane, making an angle ϕ_i with negative y-axis as shown in Fig.3.3. The field scattered from such an array in any direction in the x-y plane making an angle ϕ_s with the y-axis. Assuming that the current $I_{r'k}(z)$ induced on each element, where the subscript r'k denotes the r'k th element. For an infinite array, all the currents I are equal in magnitude and have a linear phase delay matching that of the incident wave (Floquet's theorem). The array is assumed to be sufficiently large (R'', $K >> 1$) so that it can be considered as a truncated version of an infinite array. The r'k th element current can be written as

$$I_{r'k}(z) = I_{00}(z) \exp(-j\beta k D_x \sin\phi_i) \tag{A.1}$$

where $\beta = 2\pi/\lambda$ is the phase constant. Assuming

$$I_{00}(z) = I_{00}^{s} f(z) + I_{00}^{t} g(z) \tag{A.2}$$

where $f(0) = g(0) = 1$, so that the current at the terminals of the 00^{th} element is

$$I_{00}(0) = I_{00}^{s} + I_{00}^{t} \tag{A.3}$$

The compensation theorem of the circuit theory can be used to find I_{00}^{s} and I_{00}^{t} in the following way. Assuming I_{00}^{s} is the current at the terminals with the terminals short circuited, then I_{00}^{t} is the current due to an emf of - $I_{00}(0)Z_L$ applied to the terminals. In other words, the terminal current I_{00}^{s} is induced when the array functions as a passive scatterer with all of its elements short circuited, whereas the terminal current I_{00}^{t} is induced when the array functions as an active transmitter. Thus

$$I_{00}(0) = I_{00}^{\,s}(0) - \frac{Z_L I_{00}(0)}{Z_A} \tag{A.4}$$

where $Z_A = R_A + jX_A$ is the driving point impedance of an element of this array and Z_L is the load impedance. When the array is scanned to the direction ϕ_{i_0} it follows from eqn. A.2 and eqn. A.4 that

$$I_{00}(z) = I_{00}(0)\left[\frac{Z_L + Z_A}{Z_A} f(z) - \frac{Z_L}{Z_A} g(z)\right] \tag{A.5}$$

In designing of the resonant screens, it has been observed that the best results are obtained when the linear elements are shorter than one wavelength in the frequency band of interest. For this case $f(z)$ and $g(z)$ can be written as

$$f(z) = \frac{(\cos \beta z - \cos \beta l_e)}{(1 - \cos \beta l_e)} \tag{A.6a}$$

$$g(z) = \frac{\sin \beta\,(l_e - |z|\,)}{\sin \beta l_e} \tag{A.6b}$$

to a good approximation where $2l_e = 2\,(l + \Delta\, l)$ (i.e. a length somewhat exceeding the physical

length $2l$). Thus effective length is introduced by the end capacitance of the linear elements; expressions for l_e are given in several antenna books. In addition to the restriction on length just mentioned, the elements should not be spaced too closely ($D_x > 0.2\ \lambda$, $D_z > 0.2\ \lambda$).

In eqn. A.5 the driving point impedance Z_A is found from the theory of antenna arrays. It remains to determine $I_{00}\ (0)$. In the present case only magnitude of the reflection coefficient, R' is determined; hence only the magnitude of $I_{00}\ (0)$ is needed.

Assuming that the array of loaded elements be exposed to an incident plane wave as described in the first paragraph. Each element, except for those at the edge, will absorb the same fraction of the total received P_{max}^{A} under matched condition.

$$P_{\max}^{E} = \frac{P_{\max}^{A}}{N} = \frac{\lambda^2}{4\pi N} G S_i \qquad \text{(A.7)}$$

where the total number of elements N is $(2R''+1)\ (2K+1)$, G is the gain of the array scanned in the direction ϕ_i. Also,

$$P_{\max}^{E} = \frac{\left|V_{r'k}\right|^2}{4R_A} \qquad \text{(A.8)}$$

where V'_{rk} is the induced (or Thevenin) emf in the r'k th element. $\left|V_{r'k}\right|$ is determined from eqn. A.7 and A.8 and substituting this value into

$$I_{r'k} = \frac{V_{r'k}}{Z_A + Z_L} \qquad \text{(A.9)}$$

gives the magnitude of the current in the r'k th element.

$$\left|I_{r'k}\right| = \frac{\lambda}{\left|Z_A + Z_L\right|}\left(\frac{GR_A S_t}{\pi N}\right)^{1/2} \tag{A.10}$$

Substituting $\left|I_{00}(0)\right|$ from eqn. A.10 into eqn. A.5 and employing eqn. A.1, A.6a, and A.6b, the current on all of the elements of the array is known, except for the constant phase term noted earlier. The evaluation of the far zone scattered field and subsequently the bistatic cross section in the x-y plane is straightforward and yields

$$\sigma' = \frac{120 N R_A G \lambda^2}{\pi \left|Z_A + Z_L\right|^2}\left|F_{e1} - \frac{Z_L}{Z_A} F_{e2}\right|^2 \left[\frac{\sin\left[\left(\beta D_x/2\right)(2K+1)\left(\sin\phi_i - \sin\phi_s\right)\right]}{(2K+1)\sin\left[\left(\beta D_x/2\right)\left(\sin\phi_i - \sin\phi_s\right)\right]}\right]^2 \tag{A.11}$$

where $F_{e1} = \dfrac{\sin\beta l - \beta l_e \cos\beta l_e}{1 - \cos\beta l_e}$ (A.12)

and $F_{e2} = \dfrac{1}{\sin\beta l_e}\left[1 - \cos\beta l_e - F_{e1}\sin\beta l_e\right]$ (A.13)

This result can be further simplified. From the definition of gain and terminal impedance it can be shown with certain restrictions that

$$R_A G = 120 N\left[\frac{\cos\beta\,\Delta l - \cos\beta l_e}{\sin\beta l_e}\right]^2 \tag{A.14}$$

to a good approximation. Substituting eqn. A.14 into eqn. A.11 yields

$$\frac{\sigma'}{\lambda^2} = \frac{120^2 N^2}{\pi |Z_A + Z_L|^2} \left| F_{e1} - \frac{Z_L}{Z_A} F_{e2} \right|^2 \left[\frac{\cos \beta \Delta l - \cos \beta l_e}{\sin \beta l_e} \right]^2 \left[\frac{\sin\left[(\beta D_x / 2)(2K+1)(\sin\phi_i - \sin\phi_s) \right]}{(2K+1)\sin\left[(\beta D_x / 2)(\sin\phi_i - \sin\phi_s) \right]} \right]^2 \quad \text{(A.15)}$$

It is convenient to normalized eqn. A.15 with respect to the bistatic cross section of a flat perfectly conducting plate with the same dimensions as the array. Maximum specular scattering is desirable and it can be achieved when $\phi_i = \phi_s$. A specular reflection coefficient for the array can be defined as

$$R' = \frac{\sigma'}{\sigma_{plate}}$$

Physical optics accurately yields the specular bistatic cross section of a large perfectly conducting plate, so that from eqn A.15 it is obtained

$$R' = \frac{K(l_\lambda, l_e, Z_L, Z_A) l^4 \sec^2 \phi_i}{[D_x D_z (Z_A + Z_L)]^2} \quad \text{(A.16)}$$

where $$K(l_\lambda, l_e, Z_L, Z_A) = 3600 \frac{\left| F_{e1} - \left(\frac{Z_L}{Z_D} \right) F_{e2} \right|^2 \left[\frac{\cos \beta \Delta l - \cos \beta l_e}{\sin \beta l_e} \right]^2}{\pi^2 l_\lambda^4} \quad \text{(A.17)}$$

Eqn. A.17 can be written as

$$K(l_\lambda, l_e, Z_L, Z_A) = 3600 \frac{\left| F_{e1} - \left(\frac{Z_L}{Z_D} \right) F_{e2} \right|^2 F_{e3}^2}{\pi^2 l_\lambda^4} \quad \text{(A.18)}$$

where $F_{e3} = \dfrac{\cos\beta\,\Delta l - \cos\beta l_e}{\sin\beta l_e}$

For the *00* th element in the array, the terminal voltage V_{00} can be given as

$$V_{00} = \sum_{r'=-R''}^{R''} \sum_{k=-K}^{K} Z_{r'k} I_{r'k} \qquad \text{(A.19)}$$

Where Z'_{rk} is the mutual impedance between element *00* and the $r'k$ th element. For large arrays, the element currents are identical except for a linear phase delay (see eqn. A.1). The driving point impedance can then expressed as

$$Z_A = \frac{V_{00}}{I_{00}} = \sum_{r'=-R''}^{R''} \sum_{k=-K}^{K} \varepsilon_k Z_{r'k} \cos(\beta D_x k \sin\phi_i) \qquad \text{(A.20)}$$

where ε_k is the Neumann factor defined by

$\varepsilon_k = 1$ for $k = 0$

$= 2$ for $k \neq 0$

In the above equations, $l_\lambda = l/\lambda$, λ is the wavelength of the incident wave, $2l_e$ is the effective length of each dipole and $\Delta l = l_e - l$.

EXPRESSION FOR R_AG PRODUCT

The $R_A G$ product is derived in a manner consistent with approximations stated earlier. R_A and G are the ordinary radiation resistance and gain of the elements functioning as a transmitting array steered in the direction of incidence. Assuming that the array is steered in the direction ϕ_i the magnitude of the far-zone power density at a distance r in the direction ϕ_i can be written as

$$S_A = \frac{N|I_{00}|^2 R_A G}{4\pi r^2} \tag{A.21}$$

where I_{00} is the terminal current in the transmitting array; it is not the current given by eqn. A.9. The far-zone power density radiated by a single element in the array can be given as

$$S = \frac{\beta^2 Z_c}{16\pi^2 r^2}|I_{00}|^2\left(\int_{-l}^{l} g(z)\,dz\right)^2 \tag{A.22}$$

where Z_c is the characteristic impedance of the medium and $g(z)$ is the normalized current distribution used in eqn. A.2 and A.6b. When all of the elements of the array radiated in phase, then

$$S_A = N^2 S$$

From the preceding equations,

$$R_A G = \frac{N\beta^2 Z_C}{\pi}\left|\int_{-l}^{l} g(z)dz\right|^2 \tag{A.23}$$

Using the approximated expression for $g(z)$ given in eqn. A.6b the above eqn. can be written as

$$R_A G = 120N\left[\frac{\cos\beta\Delta l - \cos\beta l_e}{\sin\beta l_e}\right]^2 \tag{A.24}$$

ANGLE OF REFLECTION COEFFICIENT

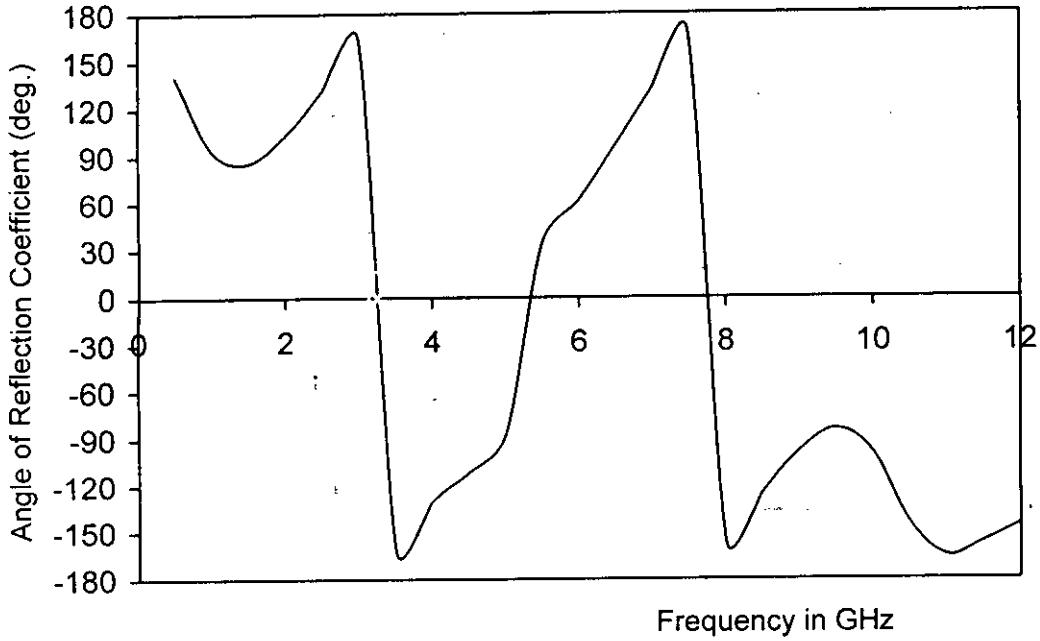

Fig. B. Angle of reflection coefficient of Fig. 4.1

APPENDIX C

RELATIVE PERMITTIVITY OF DIFFERENT DIELECTRIC MATERIALS

Dielectric materials ($\mu_r = 1.0$) have relative permittivity (ε_r) typically between 2 and 5. Relative permittivity (ε_r) for various dielectric materials is given in the following table [2],[29].

Materials	**Relative Permittivity, ε_r**
Bakelite	4.74
Mica	5.40
Neoprene	5.0-7.0
Nylon	3.50
Paper	3.00
Plexiglas	3.45
Polyethylene	2.27-2.50
Polypropylene	2.50-2.65
Polystyrene	2.56
Polyurethane	5.6-7.6
Polyvinyl chloride	3.0-8.0
Quartz	3.80
Rubber	2.5-3.0
Silicon	11.80
Silicone	3.0-3.5
Styrofoam	1.03
Teflon	2.10
Wood (dry)	1.5-4.0

RELATIONSHIP BETWEEN THE FREQUENCY AT WHICH MAXIMUM REFLECTION IS OCCURED AND DIELECTRIC CONSTANT

A best fit analysis is done by computer software package Micor-Cal Origin™ to obtain a relationship between the frequency (f_{rmax}) at which maximum reflection is occurred and ε_r. The best fit plot is shown in Fig. D. The relationship is given as

$$f_{r\max} = 6.87753 + 0.25332\varepsilon_r - 0.12516\varepsilon_r^2$$

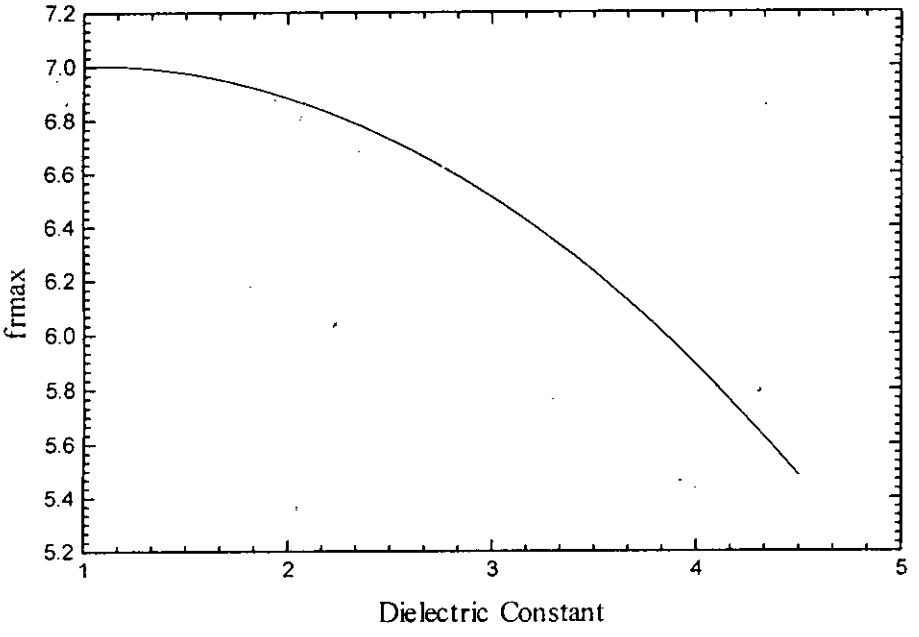

Fig. D. A best fit plot of frequency at maximum reflection versus ε_r.

COMPUTER PROGRAMS

```
/*
-------------------------------------------------------------------------------
    This is a program that has been written in C++ language for the
calculation of the Reflection Coefficient of a Frequency Selective Surface
(FSS) of loaded dipoles on a dielectric substrate.
-------------------------------------------------------------------------------
                                                                              */
#include <complex.h>
#include <iostream.h>
#include <stdio.h>
#include <math.h>
#include <float.h>
#include <stdlib.h>
#include <string.h>
#include <conio.h>

#define c 3.0e8          /* Speed of EM wave in free space(meter/sec)*/
#define PI 3.141593
#define llt 0.0
#define epsi0 8.854e-12  /* Permittivity of free space(farad/meter)*/
#define mu0 12.57e-7     /* Permeability of free space(henry/meter)*/

      static float beta;
      static float omega;
      static float l;
      static float width;
      static float le;
      static float Dx;
      static float Dz;
      static float wavelength;
      static float deltal;
      static float phi_inc;
      static float mu;
      static float mur;
      static float epsi;
      static float epsir;
      static float epsire;
      static float epsirel;
      static float epsire2;

      static int no_rows;
      static int no_cols;
      static int i;
      static int j;

      long double pow(long double(x),long double (y));

void main()
{

      int ang_inc;
```

```
float Rl,Xl,R,pha_velocity;
float K(float,float,complex);
complex driv_impedance(void);

int FileNum=1;
FILE *fp;
char FileName[20]="Reflec",FileName3[6]=".dat",FileName2[5];


clrscr();
do{
printf("\nStarting file # %d\n",FileNum);
itoa(FileNum,FileName2,10);
strcat(FileName,FileName2);
strcat(FileName,FileName3);

fp=fopen(FileName,"w");

fprintf(fp,"\t\t THIS IS THE OUTPUT OF THE PROGRAM FSS.CPP\n");
fprintf(fp,"\t\t\t output file name: %s\n",FileName);
fprintf(fp,"\t\t\t-------------------------------\n\n");

printf(" Input the nos. of rows in the array, no_rows    =\t");
scanf("%d",& no_rows);
fprintf(fp,"\t\t number of rows     =%d\n",no_rows);

printf(" Input the nos. of columns in the array, no_cols =\t");
scanf("%d",& no_cols);
fprintf(fp,"\t\t number of columns  =%d\n\n",no_cols);

printf(" Input the resistance of the load,Rl   =\t");
scanf("%f",&Rl);
fprintf(fp,"\t\t load resistance =%f\n",Rl);

printf(" Input the inductance of the load, Xl  =\t");
scanf("%f",&Xl);
fprintf(fp,"\t\t load inductance =%f\n\n",Xl);

      l=0.02;
      Dx=0.02;
      Dz=0.05;

fprintf(fp,"\t\t length of each dipole(m) =%f\n",2*l);
fprintf(fp,"\t\t horizontal spacing(m)    =%f\n",Dx);
fprintf(fp,"\t\t vertical spacing(m)      =%f\n\n",Dz);

float llambda,s,w,h,k;

/*  Calculation of the effective dielectric constant, epsire   */

      mur=1.0;
      mu =mur*mu0;

fprintf(fp,"\t permeability of the dielectric substrate=%f\n",mu);
printf(" Input relative permittivity of the substrate,epsir=\t");
scanf("%f",& epsir);
fprintf(fp,"\t relatve permittivity of the substrate =%f\n\n",epsir);

      s=Dx;
      w= 0.02*l;
```

```
            h= 0.001;
            k=s/(s+2.0*w);

        fprintf(fp,"\t thickness of the dielectric substrate(m)=%f\n",h);

        epsire1= tan(h)*(0.775*log(h/w)+1.75);
        epsire2= (k*w*(0.04-0.7*k+0.01*(1.0-0.1*epsir)*(0.25+k)))/h;
        epsire = ((epsir+1.0)*(epsire1+epsire2))/2.0;

        epsi = epsi0*epsire;

fprintf(fp,"\t effective dielectric constant of medium=%f\n\n", epsire);
fprintf(fp,"\t permittivity of the equivalent medium =%.4e\n\n", epsi);

   for(ang_inc=1;ang_inc<=6;ang_inc++)
   {

printf(" \n for incidence angle (degree) =%d\n\n",15*ang_inc);
fprintf(fp," \n for incidence angle(degree) =%d\n\n",15*ang_inc);

printf(" Freq(GHz)\t\Reflection Coeff.\n\n ");
fprintf(fp," Freq(GHz)\t\Reflection Coeff.\n\n ");

            phi_inc=15*ang_inc*PI/180.0;
            pha_velocity=c/sqrt(mur*epsire);
            deltal=0.3*l;
            le=l+deltal;

        float incr;
        float freqGHz=0.0;

        do
        {
        incr=0.5;
        freqGHz=freqGHz+incr;

                    wavelength= pha_velocity/(freqGHz*1.0e9);
                    omega=2.0*PI*freqGHz*1.0e9;
                    beta=2.0*PI/wavelength;
                    complex Zl= complex(Rl,omega*Xl);
                    llambda=l/wavelength;

/*  Calculation of the reflection coefficient, R   */

        complex x1=driv_impedance();
        float x2=K(llambda,le,Zl);

              R=(x2* pow(1,4))/(pow((Dx*Dz),2)*
              pow(abs(x1+Zl),2)*pow(cos(phi_inc),2));

        printf("\t%.2f\t\%f\n",freqGHz,R);
        fprintf(fp,"\t%.2f\t\%f\n",freqGHz,R);

        } while(freqGHz<12);
             }

        strcpy(FileName,"Reflec");
        FileNum++;
        fclose(fp);
        }while(FileNum<2);
```

```
      printf("end of the program\n");
}

/*-------------------------------------------------------------------------*/

/*   Calculation of the value of K   */

float K(float llambda,float le,complex Zl)
{
      complex driv_impedance(void);

      float Fe1=(sin(beta*l)-beta*l*cos(beta*le))/(1-cos(beta*le));
      float Fe2=(1-cos(beta*le)-Fe1*sin(beta*le))/sin(beta*le);
      float Fe3=(cos(beta*deltal)-cos(beta*le))/sin(beta*le);
      complex xxx=driv_impedance();
      return(3600*pow(abs(Fe1-Fe2*Zl/xxx),2)*pow(Fe3,2))/
            (PI*PI*pow(llambda,4));
}

/*   Calculation of the driving point impedance(Za)   */

complex driv_impedance(void)
{
      int epsiok,m,n;
      complex Za;
      complex self_impedance(void);
      complex xxx,mutual_impedance(void);

      m = (no_rows)/2;
      n = (no_cols)/2;
      Za=complex(0.0,0.0);
      xxx=mutual_impedance();

      for(i=-m;i<=m;i++)
            {
                  for(j=-n;j<=n;j++)
                  {
                  if(j==0) epsiok=1;
                  else epsiok=2;

                  float cs=cos(beta*Dx*j*sin(phi_inc));
                  Za+=epsiok* xxx*cs;
                  }
                  }
      cout << "real part of Za =  " << real(Za) << " \n";
      cout << "imaginary part of Za = " << imag(Za) << "\n";
      getchar();

      return Za;
}

/*   Calculation of the mutual impedance   */

complex mutual_impedance(void)
{
      complex ff1(float);
      complex ff2(float);
      complex self_impedance(void);
      complex parallel(float);
```

```
        complex compl_intg(complex(*fu)(float),float,float);
        float potscalar,potvector;

        potscalar=beta/(8.0*PI*omega*epsi*sin(beta*le)*sin(beta*le));
        potvector=-omega*mu/(8.0*PI*sin(beta*le)*sin(beta*le));

        if((j==0)&&(i==0)) return self_impedance();
        else if ((i==0)&&(j!=0))
             {
        return parallel(j*Dx);
        }
        else{

        complex c1=compl_intg(ff1,(i*Dz-1),(i*Dz+1));
        complex c2=compl_intg(ff2,(i*Dz-1),(i*Dz+1));
        return complex(0.0,1.0)*potscalar*c1+potvector*c2;
            }
}

/*-------------------------------------------------------------------------*/

complex ff1(float z)
{
        complex f1(float);
        complex differentiate (complex (*fu)(float),float);
        return differentiate(f1,z)*sin(beta*(le-fabs(z)));
}

        static float z1;
        static float z2;

complex f1(float z)
{
        z1=z;
        complex Eirsp(float);
        complex compl_intg(complex(*fu)(float),float,float);
        return compl_intg(Eirsp,-1,1);
}

complex ff2(float z)
{
        z2=z;
        complex Eirvp(float);
        complex compl_intg(complex(*fu)(float),float,float);
        return sin(beta*(le-fabs(z)))*compl_intg(Eirvp,-1,1);
}

complex Eirsp(float zprime)
{
        complex bet=complex(0.0,beta);
        float dist=sqrt(j*Dx*j*Dx+(z1-zprime)*(z1-zprime));
        complex retplus=-bet*(le-fabs(zprime)+dist);
        complex retminus=bet*(le-fabs(zprime)-dist);
        return (exp(retplus)+exp(retminus))/dist;
}


complex Eirvp(float zprime)
{
```

```
        complex bet=complex(0.0,beta);
        float dist=sqrt(j*Dx*j*Dx+(z2-zprime)*(z2-zprime));
        complex retplus=-bet*(le-fabs(zprime)+dist);
        complex retminus=bet*(le-fabs(zprime)-dist);
        return (exp(retplus)-exp(retminus))/dist;
}
/*-------------------------------------------------------------------------*/

/*   Calculation of the self-impedance (Z11)     */

complex self_impedance(void)
{
        complex prod,Z11;
        complex S(float);
        complex C(float);

        prod=complex(0.0,60.0)/(sin(beta*l)*sin(beta*l));
        Z11 =prod*(4.0*cos(beta*l)*cos(beta*l)*S(beta*l)
             -cos(2.0*beta*l)*S(2.0*beta*l)
             -sin(2.0*beta*l)*(2.0*C(beta*l)-C(2.0*beta*l)));
        return Z11;
}
/*-------------------------------------------------------------------------*/

float intg(float(*fu)(float),float a,float b)
{
        int jj;
        float xr,xm,dx;
        double s;

        static float xx[]={0.0,0.1488743389,0.4333953941,
                           0.6794095682,0.8650633666,0.97390652};
        static float ww[]={0.0,0.2955242247,0.2692667193,
                           0.2190863625,0.1494513491,0.06667134};

              xm=0.5*(b+a);
              xr=0.5*(b-a);
              s=0.0;

        for(jj=1;jj<=5;jj++){
        dx=xr*xx[jj];
        s+=ww[jj]*((*fu)(xm+dx)+(*fu)(xm-dx));
        }
        return s*=xr;
}

float Cin(float x)
{
        float cinc(float);
        if(x==0.0)return 0.0;
        else  {
        return intg(cinc,1lt,x);
              }
}

float Cii(float x)
{
        float cinc(float);
```

```
        if(x==0.0)return 0.0;
        else  {
        return 0.577+log(x)-intg(cinc,llt,x);
              }
}

float Sii(float x)
{
        float sinc(float);
        if(x==0.0) return 0.0;
        else  {
        return intg(sinc,llt,x);
              }
}

complex C(float B)
{
        float Cin(float),Sii(float);

        float w=0.01*2*1;
        float t=w/7.3;

        float width=0.25*w*(1+t*(1+log((4*PI*w)/t))/(PI*w));
        return log(2.0*1/width)
               -0.5*Cin(2.0*B)
               -complex(0.0,0.5)*Sii(2.0*B);
}

complex S(float B)
{
        float Cin(float),Sii(float);
        return-beta*width
              -complex(0.0,0.5)*Cin(2.0*B)
              +0.5*Sii(2.0*B);
}

float sinc(float x)
{
        return sin(x)/x;
}

float cinc(float x)
{
        return (1-cos(x))/x;
}

/*-------------------------------------------------------------------------*/

        static float argm1;
        static float argm2;
        static float argm3;
        static float argm4;

complex parallel(float d)
{
        float Rpa(float);
        float Xpa(float);
        float mult=30.0/(sin(beta*1)*sin(beta*1));
        return mult*complex(Rpa(d),Xpa(d));
}
```

```
float Rpa(float d)
{
      argm1=beta*(sqrt(d*d+1*1)-1);
      argm2=beta*(sqrt(d*d+1*1)+1);
      argm3=beta*(sqrt(d*d+4.0*1*1)-2.0*1);
      argm4=beta*(sqrt(d*d+4.0*1*1)+2.0*1);

      float cicos=cos(beta*1*(Cii(argm1)+Cii(argm2)));

      return 2.0*(2.0+cos(2.0*beta*1))*Cii(beta*d)
            -4.0*cicos*cicos+cos(beta*2.0*1*(Cii(argm3)+Cii(argm4)))
            +sin(beta*2.0*1*(Sii(argm4)-Sii(argm3)
            -2.0*Sii(argm2)+2.0*Sii(argm1)));
}

float Xpa(float d)
{
      float sicos=cos(beta*1*(Sii(argm1)+Sii(argm2)));

      return  -2.0*(2.0+cos(2.0*beta*1))*Sii(beta*d)
            +4.0*sicos*sicos-cos(beta*2.0*1*(Sii(argm3)+Sii(argm4)))
            +sin(beta*2.0*1*(Cii(argm4)-Cii(argm3)
            -2.0*Cii(argm2)+2.0*Cii(argm1)));
}

/*-------------------------------------------------------------------------*/

/*   Numerical integration of a complex function     */

complex compl_intg(complex(*fu)(float),float a,float b)
{
      int jj;
      float xr,xm,dx;
      complex s;

      static float xx[]={0.0,0.1488743389,0.433953941,
                         0.6794095682,0.8650633666,0.97390652};
      static float ww[]={0.0,0.2955242247,0.2692667193,
                         0.2190863625,0.1494513491,0.06667134};

      xm=0.5*(b+a);
      xr=0.5*(b-a);

      s=complex(0.0,0.0);

      for(jj=1;jj<=5;jj++)
            {
            dx=xr*xx[jj];
            s+=ww[jj]*((*fu)(xm+dx)+(*fu)(xm-dx));
            }
      return s*=xr;
}

/*-------------------------------------------------------------------------*/

/*  Numerical integration of a complex function (exponential type) */

complex EiIntg(float x)
{
```

```
        int t,todd,teven,lim,fact(int);
        float gamma,si,ci,ssum,csum;

        ssum=0.0;

        if(x==0.0)return complex(1.0,0.0);
        else{
            gamma=0.577+log(fabs(x));
            csum=gamma;
        if(x<0.2)
            {
            si=x;
            ci=gamma;
            }
        else if(x>1)
            {
            si=PI/2.0-cos(x)/x;
            ci=sin(x)/x;
            }
        else
            {
            lim=3;
        for(t=1;t<=lim;t++)
            {
            todd=2*t-1;
            teven=2*t;
            ssum+=pow(-1.0,(t-1))*pow(x,todd)/(todd*fact(todd));
            csum+=pow(-1.0,(t-1))*pow(x,teven)/(teven*fact(teven));
            }
        si=ssum;
        ci=csum;
        }
        return complex(ci,si);
        }
}

/*-------------------------------------------------------------------------*/

/*   calculation of the factorial (n!)  */

int fact(int g)
{
        int n;
        int fac=1;
        if(g==0) fac=1;
        else
            {
            for(n=1;n<=g;n++)
                {
                fac*=n;
                }
            }

        return fac;
}

/*-------------------------------------------------------------------------*/

/*  Numerical differentiation of a complex function   */
```

```
#define nval 6
#define tol .00001

      static float hh=0.005;

complex differentiate (complex (*func)(float),float z)
{
      int ii;
      float h=hh;
      complex DD[20];
      float EE[20],RR[20];

      DD[0]=(func(z+h)-func(z-h))/(2.0*h);

      for(ii=1;ii<=2;ii++)
            {
            h= h/2.0;
            DD[ii]=(func(z+h)-func(z-h))/(2.0*h);
            EE[ii]=abs(DD[ii]-DD[ii-1]);
            RR[ii]=2.0*EE[ii]/(abs(DD[ii])+abs(DD[ii-1])+tol);
            }
      ii=1;
      while((EE[ii]>EE[ii+1])&&(ii<nval))
            {
            h=h/2.0;
            DD[ii+2]=(func(z+h)-func(z-h))/(2.0*h);
            EE[ii+2]=abs(DD[ii+2]-DD[ii+1]);
            RR[ii+2]=2.0*EE[ii+2]/(abs(DD[ii+2])+abs(DD[ii+1])+tol);
            ii++;
            }
      return DD[ii];
}
```

```
/*
-------------------------------------------------------------------------
    This is a program that has been written in C++ language for the
calculation of the Reflection Coefficient and Absorption Loss of a Frequency
Selective Surface (FSS) of square loops on a dielectric substrate.
-------------------------------------------------------------------------
                                                                        */

#include <complex.h>
#include <iostream.h>
#include <stdio.h>
#include <math.h>
#include <float.h>
#include <stdlib.h>
#include <string.h>
#include <conio.h>

#define c 3.0e8        /* Speed of EM wave in free space(meter/sec)*/
#define PI 3.141593
#define llt 0.0
#define epsi0 8.854e-12 /* Permittivity of free space(farad/meter)*/
#define mu0 12.57e-7    /* Permeability of free space(henry/meter)*/

      static float beta;
      static float omega;
      static float l;
      static float width;
      static float le;
      static float Dx1,Dx2;
      static float Dz1,Dz2;
      static float wavelength;
      static float deltal;
      static float phi_inc;
      static float mu;
      static float mur;
      static float epsi;
      static float epsir;
      static float epsire;
      static float epsire1;
      static float epsire2;

      static int no_rows;
      static int no_cols;
      static int i;
      static int j;

      long double pow(long double(x),long double (y));

void main()
{

      int ang_inc;
      float R,R1,R2,pha_velocity;
      float K1(float,float,complex),K2(float,float,complex);
      complex driv_impedance1(void),driv_impedance2(void);

      int FileNum=1;
```

```
FILE *fp;
char FileName[20]="Reflec",FileName3[6]=".dat",FileName2[5];


clrscr();
do{
printf("\nStarting file # %d\n",FileNum);
itoa(FileNum,FileName2,10);
strcat(FileName,FileName2);
strcat(FileName,FileName3);

fp=fopen(FileName,"w");

fprintf(fp,"\t\t THIS IS THE OUTPUT OF THE PROGRAM FSS.CPP\n");
fprintf(fp,"\t\t\t output file name: %s\n",FileName);
fprintf(fp,"\t\t\t--------------------------------\n\n");

printf(" Input the nos. of rows in the array, no_rows    =\t");
scanf("%d",& no_rows);
fprintf(fp,"\t\t number of rows     =%d\n",no_rows);

printf(" Input the nos. of columns in the array, no_cols =\t");
scanf("%d",& no_cols);
fprintf(fp,"\t\t number of columns  =%d\n\n",no_cols);

      l=0.02;
      Dx1=Dz2=0.01;
      Dz1=Dx2=0.02;

fprintf(fp,"\t\t length of each side of square loop (m) =%f\n",l/2);
fprintf(fp,"\t\t horizontal spacing(m)    =%f\n",Dx1);
fprintf(fp,"\t\t vertical spacing(m)      =%f\n\n",Dz1);

float llambda,s,w,h,k;

/*  Calculation of the effective dielectric constant, epsire   */

      mur=1.0;
      mu =mur*mu0;

fprintf(fp,"\t permeability of the dielectric substrate=%f\n",mu);

printf(" Input relative permittivity of the substrate,epsir=\t");
scanf("%f",& epsir);
fprintf(fp,"\t relatve permittivity of the substrate   =%f\n\n",epsir);

      s=Dx1;
      w= 0.02*l;
      h= 0.001;
      k=s/(s+2.0*w);

fprintf(fp,"\t thickness of the dielectric substrate(m)=%f\n",h);

epsire1= tan(h)*(0.775*log(h/w)+1.75);
epsire2= (k*w*(0.04-0.7*k+0.01*(1.0-0.1*epsir)*(0.25+k)))/h;
epsire = ((epsir+1.0)*(epsire1+epsire2))/2.0;

epsi = epsi0*epsire;

fprintf(fp,"\t effective dielectric constant of medium =%f\n\n",epsire);
```

```
fprintf(fp,"\t permittivity of the equivalent medium =%.4e\n\n",epsi);

for(ang_inc=1;ang_inc<=6;ang_inc++)
{

   printf(" \n for incidence angle (degree) =%d\n\n",15*ang_inc);
   fprintf(fp," \n for incidence angle(degree) =%d\n\n",15*ang_inc);

   printf(" Freq(GHz)\t\Reflection Coeff.\t\Absorption loss\n\n ");
   fprintf(fp," Freq(GHz)\t\Reflection Coeff.\t\Absorption loss\n\n ");

         phi_inc=15*ang_inc*PI/180.0;
         pha_velocity=c/sqrt(mur*epsire);
         deltal=0.3*l;
         le=l+deltal;

   float incr;
   float freqGHz=0.0;

   do
   {
   incr=0.5;
   freqGHz=freqGHz+incr;

               wavelength= pha_velocity/(freqGHz*1.0e9);
               omega=2.0*PI*freqGHz*1.0e9;
               beta=2.0*PI/wavelength;
               complex Z1= complex(0.0,0.0);
               llambda=l/wavelength;

   float loop_resistance,AL,absorption_loss;

   int no_loops=25;
   float loop_perimeter=2*l;
   float sigma=5.8e7;
   float a=width;

/*  Calculation of the reflection coefficient and absorption loss  */

   complex x1=driv_impedance1();
   float x2=K1(llambda,le,Z1);
   complex x3=driv_impedance2();
   float x4=K2(llambda,le,Z1);
   complex x5=induced_voltage();

         R1=(x2* pow(l,4))/(pow((Dx1*Dz1),2)*
         pow(abs(x1+Z1),2)*pow(cos(phi_inc),2));

         R2=(x4* pow(l,4))/(pow((Dx2*Dz2),2)*
         pow(abs(x3+Z1),2)*pow(sin(phi_inc),2));

         R= R1+R2;

         loop_resistance= (loop_perimeter/(2*a))*
                     sqrt((freqGHz*1.0e9*mu0)/(PI*sigma));
         AL=(pow(abs(x5),2))/loop_resistance;
         absorption_loss=10*log(AL*no_loops);

   printf("\t%.2f\t\%f\t\%f\n",freqGHz,R,absorption_loss);
   fprintf(fp,"\t%.2f\t\%f\t\%f\n",freqGHz,R,absorption_loss);
```

```
      } while(freqGHz<12);
            }

      strcpy(FileName,"Reflec");
      FileNum++;
      fclose(fp);
      }while(FileNum<2);
      printf("end of the program\n");
}

/*-------------------------------------------------------------------------*/

/*   Calculation of the value of K   */

float K1(float llambda,float le,complex Z1)
{
      complex driv_impedance1(void);

      float Fe1=(sin(beta*l)-beta*l*cos(beta*le))/(1-cos(beta*le));
      float Fe2=(1-cos(beta*le)-Fe1*sin(beta*le))/sin(beta*le);
      float Fe3=(cos(beta*deltal)-cos(beta*le))/sin(beta*le);

      complex xxx1=driv_impedance1();
      return(3600*pow(abs(Fe1-Fe2*Z1/xxx1),2)*pow(Fe3,2))/
            (PI*PI*pow(llambda,4));
}

float K2(float llambda,float le,complex Z1)
{
      complex driv_impedance2(void);

      float Fe1=(sin(beta*l)-beta*l*cos(beta*le))/(1-cos(beta*le));
      float Fe2=(1-cos(beta*le)-Fe1*sin(beta*le))/sin(beta*le);
      float Fe3=(cos(beta*deltal)-cos(beta*le))/sin(beta*le);

      complex xxx2=driv_impedance2();
      return(3600*pow(abs(Fe1-Fe2*Z1/xxx2),2)*pow(Fe3,2))/
            (PI*PI*pow(llambda,4));
}
/*   Calculation of the driving point impedance(Za)   */

complex driv_impedance1(void)
{
      int epsiok,m,n;
      complex Za1;
      complex self_impedance(void);
      complex xxx1,mutual_impedance1(void);

      m = (no_rows-1)/2;
      n = (no_cols-1)/2;
      Za1=complex(0.0,0.0);
      xxx1=mutual_impedance1();

      for(i=-m;i<=m+1;i++)
            {
                  for(j=-n;j<=n+1;j++)
                  {
                  if(j==0) epsiok=1;
                  else epsiok=2;
```

```
                    float cs1=cos(beta*Dx1*j*sin(phi_inc));
                    Za1+=epsiok* xxx1*cs1;
                    }
              }
        return Za1;
}

complex driv_impedance2(void)
{
        int epsiok,m,n;
        complex Za2;
        complex self_impedance(void);
        complex xxx2,mutual_impedance2(void);

        m = (no_rows-1)/2;
        n = (no_cols-1)/2;
        Za2=complex(0.0,0.0);
        xxx2=mutual_impedance2();

        for(i=-m;i<=m+1;i++)
             {
                    for(j=-n;j<=n+1;j++)
                    {
                    if(j==0) epsiok=1;
                    else epsiok=2;

                    float cs2=cos(beta*Dz2*j*cos(phi_inc));
                    Za2+=epsiok* xxx2*cs2;
                    }
              }
        return Za2;
}

/*   Calculation of the mutual impedance    */

complex mutual_impedance1(void)
{
        complex ff1(float);
        complex self_impedance(void);
        complex parallel(float);

        complex compl_intg(complex(*fu)(float),float,float);
        float potvector;

        potvector=-omega*mu/(8.0*PI*sin(beta*le)*sin(beta*le));

        if((j==0)&&(i==0)) return self_impedance();
        else if ((i==0)&&(j!=0))
              {
        return parallel(j*Dx1);
        }
        else{

        complex c1=compl_intg(ff1,(i*Dz1),(i*Dz1+2*l));
        return potvector*c1;
            }
}

        static float z1;
```

```
complex ff1(float z)
{
      z1=z;
      complex Eirvp1(float);
      complex compl_intg(complex(*fu)(float),float,float);
      return sin(beta*(le-fabs(z)))*compl_intg(Eirvp1,0,2*l);
}

complex Eirvp1(float zprime)
{
      complex bet=complex(0.0,beta);
      float dist=sqrt(j*Dx1*j*Dx1+(z1-zprime)*(z1-zprime));
      complex retplus=-bet*(le-fabs(zprime)+dist);
      complex retminus=bet*(le-fabs(zprime)-dist);
      return (exp(retplus)-exp(retminus))/dist;
}

complex mutual_impedance2(void)
{
      complex ff2(float);
      complex self_impedance(void);
      complex parallel(float);

      complex compl_intg(complex(*fu)(float),float,float);
      float potvector;

      potvector=-omega*mu/(8.0*PI*sin(beta*le)*sin(beta*le));

      if((j==0)&&(i==0)) return self_impedance();
      else if ((i==0)&&(j!=0))
            {
      return parallel(j*Dz2);
      }
      else{

      complex c2=compl_intg(ff2,(i*Dx2),(i*Dx2+2*l));
      return potvector*c2;
          }
}

      static float x1;

complex ff2(float x)
{
      x1=x;
      complex Eirvp2(float);
      complex compl_intg(complex(*fu)(float),float,float);
      return sin(beta*(le-fabs(x)))*compl_intg(Eirvp2,0,2*l);
}

complex Eirvp2(float xprime)
{
      complex bet=complex(0.0,beta);
      float dist=sqrt(j*Dz2*j*Dz2+(x1-xprime)*(x1-xprime));
      complex retplus=-bet*(le-fabs(xprime)+dist);
      complex retminus=bet*(le-fabs(xprime)-dist);
      return (exp(retplus)-exp(retminus))/dist;
}
```

```
/*-------------------------------------------------------------------------*/

complex induced_voltage(void)
{
      float potvector;
      complex xxx1,mutual_impedance1(void);
      xxx1=mutual_impedance1();
      potvector=-omega*mu/(8.0*PI*sin(beta*le)*sin(beta*le));

      return potvector*xxx1;

}

/* ------------------------------------------------------------------------*/

/*   Calculation of the self-impedance (Z11)     */

complex self_impedance(void)
{
      complex prod,Z11;
      complex S(float);
      complex C(float);

      prod=complex(0.0,60.0)/(sin(beta*l)*sin(beta*l));
      Z11=prod*(4.0*cos(beta*l)*cos(beta*l)*S(beta*l)
            -cos(2.0*beta*l)*S(2.0*beta*l)
            -sin(2.0*beta*l)*(2.0*C(beta*l)-C(2.0*beta*l)));
      return Z11;
}

/* ------------------------------------------------------------------------*/

float intg(float(*fu)(float),float a,float b)
{
      int jj;
      float xr,xm,dx;
      double s;

      static float xx[]={0.0,0.1488743389,0.4333953941,
                         0.6794095682,0.8650633666,0.97390652};
      static float ww[]={0.0,0.2955242247,0.2692667193,
                         0.2190863625,0.1494513491,0.06667134};

            xm=0.5*(b+a);
            xr=0.5*(b-a);
            s=0.0;

      for(jj=1;jj<=5;jj++){
      dx=xr*xx[jj];
      s+=ww[jj]*((*fu)(xm+dx)+(*fu)(xm-dx));
      }
      return s*=xr;
}

float Cin(float x)
{
      float cinc(float);
      if(x==0.0)return 0.0;
      else  {
      return intg(cinc,1lt,x);
```

```
            }
}

float Cii(float x)
{
      float cinc(float);
      if(x==0.0)return 0.0;
      else  {
      return 0.577+log(x)-intg(cinc,llt,x);
            }
}

float Sii(floa  x)
{
      float sinc(float);
      if(x==0.0) return 0.0;
      else  {
      return intg(sinc,llt,x);
            }
}

complex C(float B)
{
      float Cin(float),Sii(float);

      float w=0.01*2*l;
      float t=w/7.3;

      float width=0.25*w*(1+t*(1+log((4*PI*w)/t))/(PI*w));
      return log(2.0*l/width)
             -0.5*Cin(2.0*B)
             -complex(0.0,0.5)*Sii(2.0*B);
}

complex S(float B)
{
      float Cin(float),Sii(float);
      return-beta*width
            -complex(0.0,0.5)*Cin(2.0*B)
            +0.5*Sii(2.0*B);
}

float sinc(float x)
{
      return sin(x)/x;
}

float cinc(float x)
{
      return (1-cos(x))/x;
}

/*-------------------------------------------------------------------------*/

      static float argm1;
      static float argm2;
      static float argm3;
      static float argm4;

complex parallel(float d)
```

```
{
      float Rpa(float);
      float Xpa(float);
      float mult=30.0/(sin(beta*l)*sin(beta*l));
      return mult*complex(Rpa(d),Xpa(d));
}

float Rpa(float d)
{
      argm1=beta*(sqrt(d*d+l*l)-l);
      argm2=beta*(sqrt(d*d+l*l)+l);
      argm3=beta*(sqrt(d*d+4.0*l*l)-2.0*l);
      argm4=beta*(sqrt(d*d+4.0*l*l)+2.0*l);

      float cicos=cos(beta*l*(Cii(argm1)+Cii(argm2)));

      return 2.0*(2.0+cos(2.0*beta*l))*Cii(beta*d)
            -4.0*cicos*cicos+cos(beta*2.0*l*(Cii(argm3)+Cii(argm4)))
            +sin(beta*2.0*l*(Sii(argm4)-Sii(argm3)
            -2.0*Sii(argm2)+2.0*Sii(argm1)));
}

float Xpa(float d)
{
      float sicos=cos(beta*l*(Sii(argm1)+Sii(argm2)));

      return  -2.0*(2.0+cos(2.0*beta*l))*Sii(beta*d)
            +4.0*sicos*sicos-cos(beta*2.0*l*(Sii(argm3)+Sii(argm4)))
            +sin(beta*2.0*l*(Cii(argm4)-Cii(argm3)
            -2.0*Cii(argm2)+2.0*Cii(argm1)));
}
/*-------------------------------------------------------------------------*/

/*   Numerical integration of a complex function     */

complex compl_intg(complex(*fu)(float),float a,float b)
{
      int jj;
      float xr,xm,dx;
      complex s;

      static float xx[]={0.0,0.1488743389,0.433953941,
                         0.6794095682,0.8650633666,0.97390652};
      static float ww[]={0.0,0.2955242247,0.2692667193,
                         0.2190863625,0.1494513491,0.06667134};

      xm=0.5*(b+a);
      xr=0.5*(b-a);

      s=complex(0.0,0.0);

      for(jj=1;jj<=5;jj++)
            {
            dx=xr*xx[jj];
            s+=ww[jj]*((*fu)(xm+dx)+(*fu)(xm-dx));
            }
      return s*=xr;
}

/*-------------------------------------------------------------------------*/
```

```
/* Numerical integration of a complex function (exponential type) */

complex EiIntg(float x)
{
      int t,todd,teven,lim,fact(int);
      float gamma,si,ci,ssum,csum;

      ssum=0.0;

      if(x==0.0)return complex(1.0,0.0);
      else{
            gamma=0.577+log(fabs(x));
            csum=gamma;
      if(x<0.2)
            {
            si=x;
            ci=gamma;
            }
      else if(x>1)
            {
            si=PI/2.0-cos(x)/x;
            ci=sin(x)/x;
            }
      else
            {
            lim=3;
      for(t=1;t<=lim;t++)
            {
            todd=2*t-1;
            teven=2*t;
            ssum+=pow(-1.0,(t-1))*pow(x,todd)/(todd*fact(todd));
            csum+=pow(-1.0,(t-1))*pow(x,teven)/(teven*fact(teven));
            }
      si=ssum;
      ci=csum;
      }
      return complex(ci,si);
      }
}

/*-------------------------------------------------------------------------*/

/*   calculation of the factorial (n!)  */

int fact(int g)
{
      int n;
      int fac=1;
      if(g==0) fac=1;
      else
            {
            for(n=1;n<=g;n++)
                  {
                  fac*=n;
                  }
            }

      return fac;
}
```

REFERENCES

REFERENCES

[1] B. Schulz, C. Plantz and R. Brush, "Shielding Theory and Practice", *IEEE Transac. on EMC*, vol.30, no.3, pp. 187-201, August,1988.

[2] Clayton R. Paul, *Introduction to Electromagnetic Compatibility*, pp. 265-274, John Wiley & Sons, Inc., New York.

[3] J.D. Krauss, *Antennas*, McGraw-Hill, NY, pp. 257, 422-430, 1988.

[4] S.A. Schelkunoff, *Electromagnetic Waves*, New York: Van Nostrand, pp. 303-315, 1943.

[5] Pat Hanson, "Electromagnetic Compatibility", *Presentation to Institution of Engineers of Ireland*, Oct. 1992.

[6] S. Yasufuku, "Technical progress of EMI shielding materials in Japan", *IEEE Electrical Insulation Magazine*, vol.6, no.6, pp. 21-30, Nov./Dec. 1990.

[7] H. Rahman, P. K. Saha, J. Dowling and T. Curran "Shielding effectiveness measurement techniques for various materials used for EMI shielding", *IEE Colloquium on Screening of Connectors, Cables and Enclosures*, pp. 9/1-9/6, London, UK, 17 Jan. 1992.

[8] P. Hanifan, "Plating on plastics – a solution for RFI shielding", *Design Engineering*, pp. 53-59, April 1989.

[9] J. H. Ling, "Conductive coating in EMI/RFI shielding techniques", *Journal of New Electronics (GB)*, vol. 16, no. 1, pp. 29-34, 1983.

[10] B. Ballance, "Conductive engineering plastics for EMC applications", *Fourth International Conference on Plastics in Telecommunications*, London, England, 17-19 Sept., pp. 29/1-8, (London, England, Plastic and Rubber Inst.-1986).

[11] R. W. Simpson, Jr., "Flexible laminates for use in EMI shielding applications", *IEEE Electrical Insulation Magazine*, vol. 4, no. 1, pp. 11-13, Jan./ Feb. 1988.

[12] H. Rahman, J. Dowling and P.K.Saha, "Application of frequency sensitive surface in electromagnetic shielding", *Journal of Material Processing Technologies*, pp. 21-28, UK, April 1995.

[13] R. B. Kieburtz and A. Ishimaru, "Scattering by a periodically apertured conducting screen", *IRE Trans. Antennas and Propagation*, vol. AP-9, no. 5, pp. 506-514, Nov. 1961.

[14] R. H. Ott, R. G. Kouyoumjian and L. Peters Jr., "Scattering by a two dimensional periodic array of narrow plates", *Radio Science*, vol. 2 (new series), no. 11, Nov. 1967.

[15] Benedikt A. Munk, P. G. Kouyoumjian and L. Peters Jr. , "Reflection properties of periodic surfaces of loaded dipoles", *IEEE Transac. Antenna and Propagation*, vol. AP-19, no.5, pp. 612-617, Sept.1971.

[16] R. J. Luebbers and B. A. Munk, "Some effects of dielectric loading on periodic slot arrays", *IEEE Trans. Antennas and Propagation*, vol. AP-26, no. 4, pp. 536-542, July 1978.

[17] R. J. Luebbers, "Analysis of various periodic slot array geometries using modal matching", *Ph. D. Dissertation*, Dept. of Electrical Engineering, Ohio State University, Sept. 1975.

[18] Chich-Hsing Tsao and Raj Mitra, "Spetral domain analysis of frequency selective surfaces comprised of periodic arrays of crossed dipoles and jerusalem crosses', *IEEE Trans. Antennas and Propagation*, vol. AP-32, no. 5, pp. 478-486, May 1984.

[19] R. Mitra, C.H. Chen and T. Cwik, "Techniques for analyzing frequency selective surfaces- a review", *Proceedings of the IEEE*, vol. 76, no. 12, pp. 1593-1615, Dec. 1988.

[20] P. W. Grounds and K. J. Webb, "Numerical analysis of finite frequency selective surfaces with rectangular patches of various aspect ratio", *IEEE Trans. Antennas and Propagation*, vol. AP-39, no. 5, pp. 478-486, May 1991.

[21] Perry F. Wilson, Mark T. Ma, J. W. Adams, "Techniques for measuring the electromagnetic shielding effectiveness of materials: Part I:- Far- field source simulation", *IEEE Trans. on Electromagnetic Compatibility*, vol. 30, no. 3, pp. 239-250, August 1988.

[22] F. O'Nias and J. Matson, "Antenna feed system utilizing polarization independent frequency selective intermediate reflector", *U.S. Patent* 3-231-892, Jan. 1966.

[23] Theodore S. Saad, Robert C. Hansen and Gershon J. Wheeler, *Microwave Engineer's Handbook*, vol. 1, p. 119, Artech House Inc., Dedham, 1971.

[24] *The New IEEE Standard Dictionary of Electrical, Electronics and Computer Terms*, 5th Edition, Galgotia Publications Pvt. Ltd., India, 1994.

[25] P. S. Carter, " Circuit relations in radiating systems and applications to antenna problems", *Proc. IRE*, vol. 20, pp. 1004-1041, June 1932.

[26] Simon Ramo, John R. Whinnery, Theodore Van Duzer, *Fields and Waves in Communication Electronics*, Second Edition, p. 160, John Wiley & Sons, NY, 1984.

[27] G. H. Brown and R. King, "High frequency models in antenna investigations", *Proc. IRE*, vol. 22, pp. 457-480, April 1934.

[28] M. Azizul Islam, *Electromagnetic Theory*, pp. 558-568, Bangladesh (former East Pakistan) University of Engineering and Technology, Dhaka, 1969.

[29] Samuel Y. Liao, *Microwave devices and Circuits*, Third Edition, Prentice Hall of India Private Ltd., New Delhi, India, 1995.